

Topical theory talk: Electroweak baryogenesis

Yushi Mura (Osaka Univ.)

Collaborators: Kazuki Enomoto (KAIST), Shinya Kanemura (Osaka Univ.)

2023/06/23

Workshop for Tera-Scale Physics and Beyond in Hakata

Based on

K. Enomoto, S. Kanemura and Y.M, JHEP 01 (2022) 104, arXiv: 2111.13079 [hep-ph],

K. Enomoto, S. Kanemura and Y.M, JHEP 09 (2022) 121, arXiv: 2207.00060 [hep-ph],

S. Kanemura and Y.M, arXiv: 2303.11252 [hep-ph]

Introduction

- SM cannot explain Baryon Asymmetry of the Universe

From Cosmological observation, $\eta_B^{obs} = \frac{n_B - n_{\bar{B}}}{s} \simeq 8.7 \times 10^{-11}$ PDG (2022)

- Baryogenesis in the early Universe

Sakharov conditions Sakharov (1967)

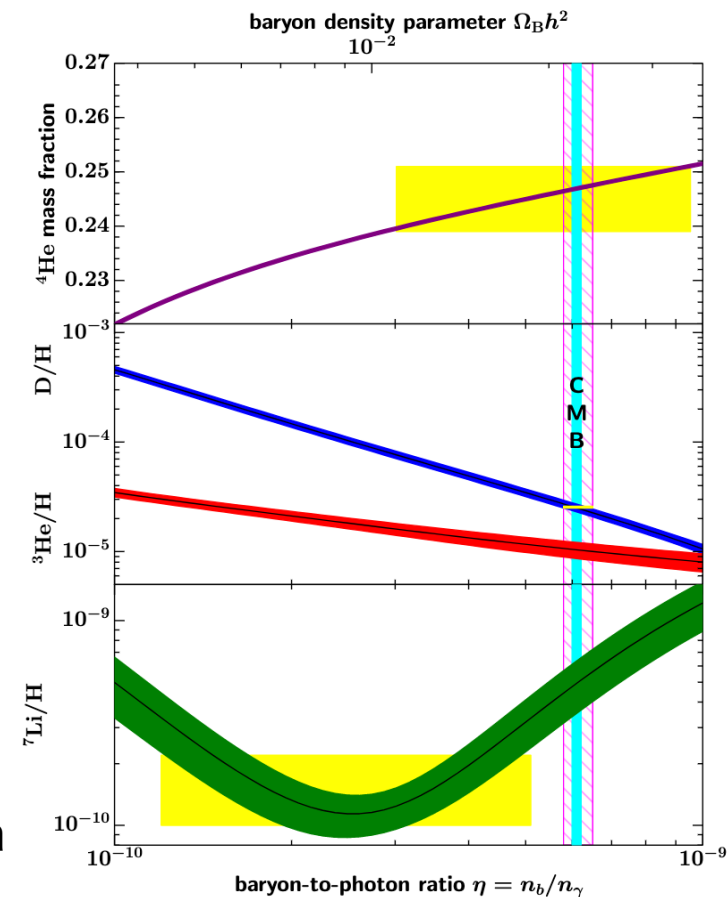
- ① Baryon number violation
- ② C and CP violation
- ③ Departure from thermal equilibrium

- Well motivated scenario

Electroweak Baryogenesis (EWBG)

- ① Sphaleron process
- ② Electroweak theory with CP violation
- ③ First order electroweak phase transition

Kuzmin, Rubakov and Shaposhnikov (1985)



Electroweak Baryogenesis

- Expanding bubble walls are created at first order PT

See Callan and Coleman (1977)

First order PT is realized by tunneling process (vacuum decay)

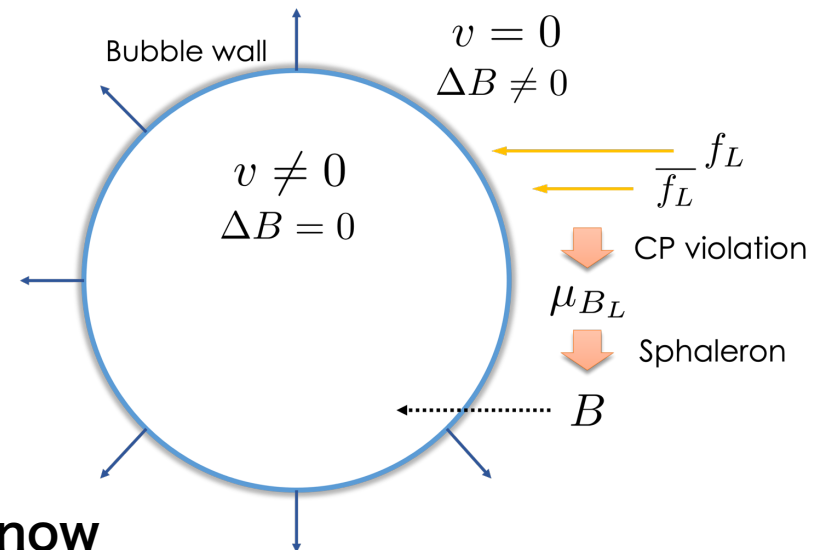
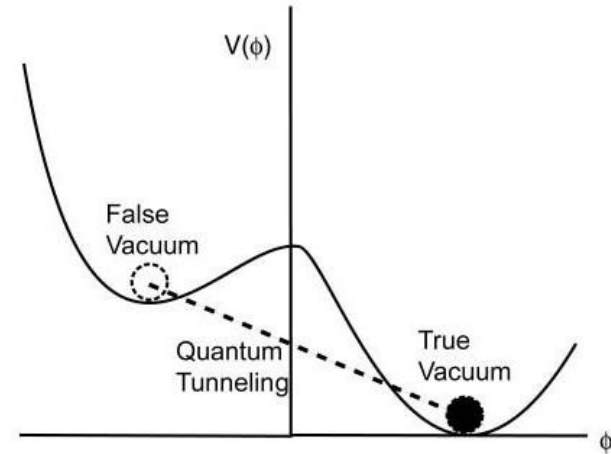
- Non-equilibrium sphaleron process around the bubble wall

$$\Gamma_{sph}^{brk}(T_n) < H(T_n) \Rightarrow v_n/T_n \gtrsim 1$$

→ Strongly first order PT

Inside : baryon number conserved
Outside : baryon number violated

- Created baryon number remains until now



Electroweak Baryogenesis

In the SM, however,

- Cross over phase transition
- Insufficient CP violation

Huet and Sather (1995)

Kajantie *et al.* (1996)



Extended Higgs sectors are needed !!

Ex)

- Singlet extended model (SM + scalar singlet)

Espinosa *et. al.* (2012); Cline and Kainulainen (2013); and more works

- Two Higgs doublet model (SM + scalar doublet)

Turok and Zadrozny (1991); Fromme, Huber and Seniuchi (2006);

Cline, Kainulainen and Trott (2011); and more works

- **Electroweak baryogenesis is just “Electroweak” physics**
- **It can be tested by many current and future experiments**

Collider, Flavor, EDM, Gravitational waves observations...

Previous studies

- Robust estimation of the BAU in two Higgs doublet model

Fromme, Huber and Seniuchi, JHEP 11 (2006) 038

Softly broken discrete (Z_2) symmetry to avoid FCNC couplings

★ corresponds to the observed BAU

- Latest bound of Electron EDM

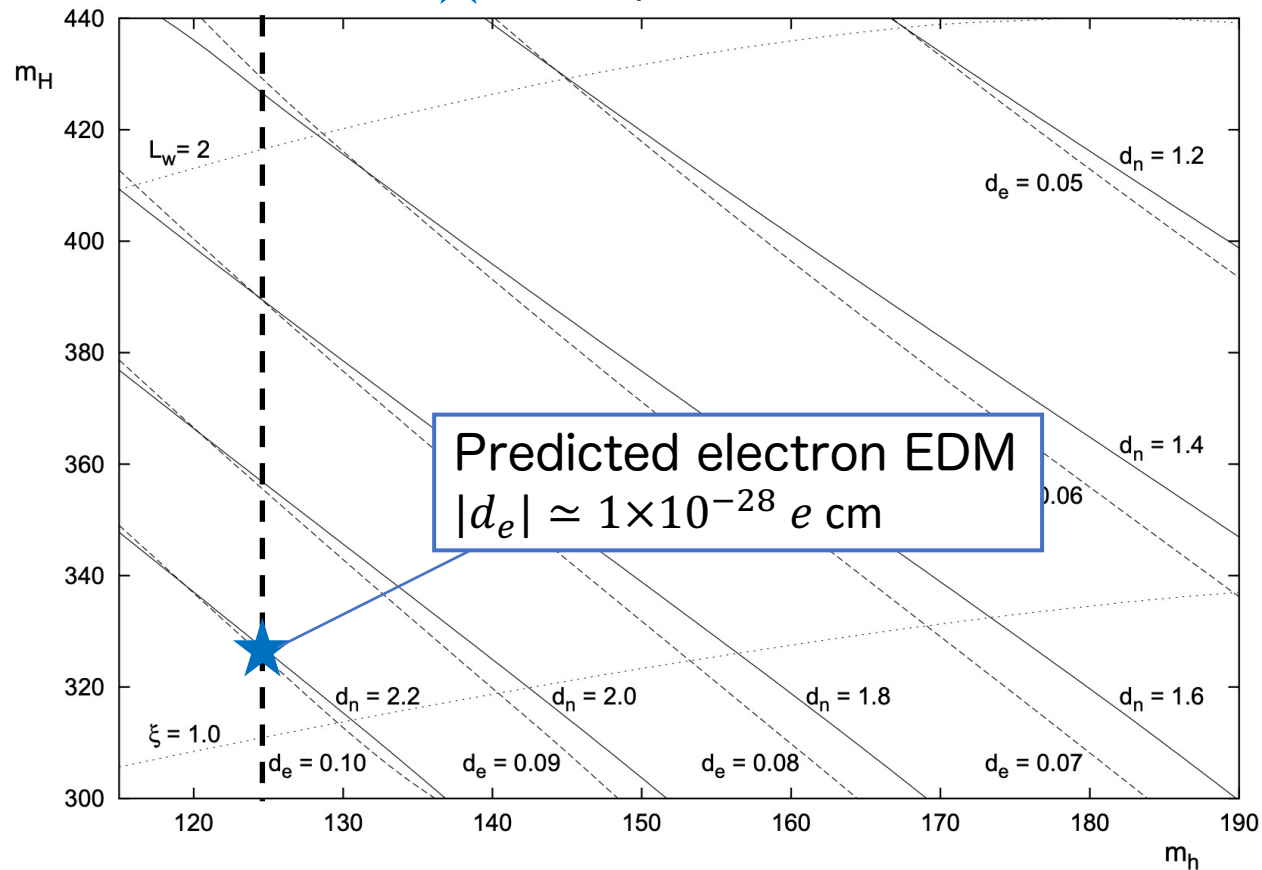
$$|d_e| < 4.1 \times 10^{-30} \text{ e cm}$$

Roussy *et al.* [Cornell Group]
arXiv:2212.11841

- Other difficulty to realize EWBG

Higgs alignment supported by LHC data

ATLAS, Nature (2022); CMS, CMS-PAS-HIG-19-005 (2020)



Aligned Two Higgs Doublet Model

- **Most general two Higgs doublet model** $\Phi_1 = \begin{pmatrix} G^+ \\ \frac{1}{\sqrt{2}}(v + h_1 + iG^0) \end{pmatrix}, \quad \Phi_2 = \begin{pmatrix} H^+ \\ \frac{1}{\sqrt{2}}(h_2 + ih_3) \end{pmatrix}$

$$V = -\mu_1^2(\Phi_1^\dagger\Phi_1) - \mu_2^2(\Phi_2^\dagger\Phi_2) - \left(\mu_3^2(\Phi_1^\dagger\Phi_2) + h.c.\right) \quad \text{Higgs basis}$$

$$+ \frac{1}{2}\lambda_1(\Phi_1^\dagger\Phi_1)^2 + \frac{1}{2}\lambda_2(\Phi_2^\dagger\Phi_2)^2 + \lambda_3(\Phi_1^\dagger\Phi_1)(\Phi_2^\dagger\Phi_2) + \lambda_4(\Phi_2^\dagger\Phi_1)(\Phi_1^\dagger\Phi_2)$$


$$+ \left\{ \left(\frac{1}{2}\lambda_5\Phi_1^\dagger\Phi_2 + \lambda_6\Phi_1^\dagger\Phi_1 + \lambda_7\Phi_2^\dagger\Phi_2 \right) \Phi_1^\dagger\Phi_2 + h.c. \right\}, \quad (\mu_3, \lambda_5, \lambda_6, \lambda_7 \in \mathbb{C})$$

Davidson and Haber (2005)

Charged scalar $m_{H^\pm}^2 = M^2 + \frac{1}{2}\lambda_3 v^2 \quad M^2 \equiv -\mu_2^2$

Neutral scalars $\mathcal{M}^2 = v^2 \begin{pmatrix} \lambda_1 & \boxed{\text{Re}\lambda_6} & -\text{Im}\lambda_6 \\ \boxed{\text{Re}\lambda_6} & \frac{M^2}{v^2} + \frac{\lambda_3 + \lambda_4 + \text{Re}\lambda_5}{2} & -\frac{1}{2}\text{Im}\lambda_5 \\ -\text{Im}\lambda_6 & -\frac{1}{2}\text{Im}\lambda_5 & \frac{M^2}{v^2} + \frac{\lambda_3 + \lambda_4 - \text{Re}\lambda_5}{2} \end{pmatrix}$

“Mixing angle among neutral scalars are small” $\Rightarrow \lambda_6 \simeq 0$



$$= \begin{pmatrix} m_h^2 & 0 & 0 \\ 0 & m_{H_2}^2 & 0 \\ 0 & 0 & m_{H_3}^2 \end{pmatrix} \quad \text{Higgs alignment}$$

- Only $\arg[\lambda_7] \equiv \theta_7$ remains in the potential

Most general Yukawa interaction

- General structure of Yukawa interaction

up-type quark

h SM Higgs

$H_{2,3}$ Additional scalars

$$-\mathcal{L}_Y = \overline{u_{i,L}} \frac{y_i \delta_{ij}}{\sqrt{2}} u_{j,R} h - \overline{u_{i,L}} \frac{\rho_{ij}}{\sqrt{2}} u_{j,R} H_2 - \overline{u_{i,L}} \frac{i\rho_{ij}}{\sqrt{2}} u_{j,R} H_3 + \text{h.c.}$$

- Small FCNC couplings related to the heavy scalars

- Consider Yukawa alignment condition

$$\rho^u = \zeta_u^* \text{diag}(y_u, y_c, y_t), \quad \rho^d = \zeta_d \text{diag}(y_d, y_s, y_b), \quad \rho^e = \zeta_e \text{diag}(y_e, y_\mu, y_\tau),$$

Pich and Tuzon (2009)

- Important particles for the BAU depends on Yukawa structure

Ex) top mass $m_t(z) = \frac{y_t}{\sqrt{2}} v(z) e^{i\theta(z)}$ generates BAU

Top transport scenario

Summary of the model

- **Alignment scenario**

One SM like Higgs and three additional scalars

- **CP violating parameters**

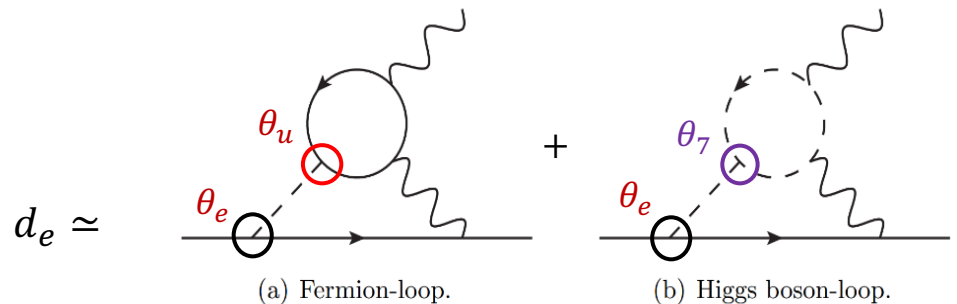
Potential $\arg[\lambda_7] \equiv \theta_7$

Yukawa $\arg[\zeta_u] \equiv \theta_u, \arg[\zeta_d] \equiv \theta_d, \arg[\zeta_e] \equiv \theta_e$

- **Electron EDM constraint**

$$|d_e| < 4.1 \times 10^{-30} e \text{ cm}$$

Roussy *et al.* [Cornell Group] [arXiv:2212.11841](https://arxiv.org/abs/2212.11841)



Kanemura, Kubota and Yagyu, JHEP 08 (2020)

- **Other experimental and theoretical constraints**

Direct detection, EW precision, EDMs, perturbative unitarity, vacuum stability and triviality bound

Baryogenesis

$$M = 30 \text{ GeV}, \lambda_2 = 0.1, |\lambda_7| = 0.8, \theta_7 = -0.9,$$

$$|\zeta_u| = |\zeta_d| = |\zeta_e| = 0.18, \theta_u = \theta_d = -2.7, \theta_e = -2.66.$$

Benchmark points

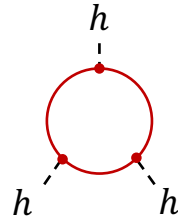
- ▼ BP1: $v_n/T_n = 2.4$
- ◆ BP2: $v_n/T_n = 2.0$

Triple Higgs coupling

Kanemura, Okada and Senaha (2005)

$$m_{\Phi}^2 = M^2 + \tilde{\lambda} v^2$$

$$\simeq \tilde{\lambda} v^2$$



- ▼ BP1 $\Delta R = 61\%$
 - ◆ BP2 $\Delta R = 44\%$
- $(\Delta R \equiv \delta\lambda_{hhh}/\lambda_{hhh}^{\text{SM}})$

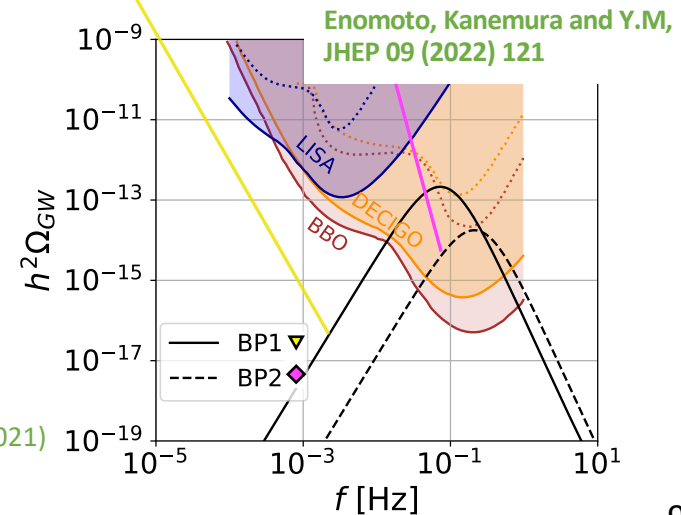
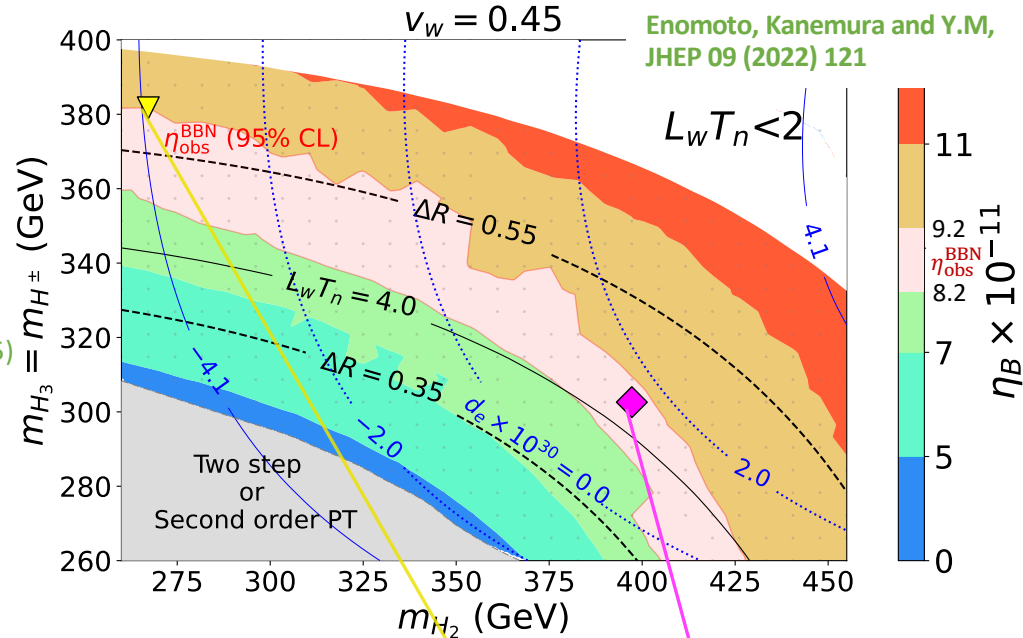
HL-LHC : 50%
 ILC 500GeV (1TeV) : 27% (10%)
 CLIC 1.4TeV (3TeV) : ~30% (~10%)

Gravitational waves

Grojean and Servant (2007);
 Kakizaki, Kanemura and Matsui (2015); and more

Peak integrated sensitivity curves Breitbach *et al.* (2019); Cline *et al.* (2021)

Future observations : LISA, DECIGO, BBO



Testing CP violation

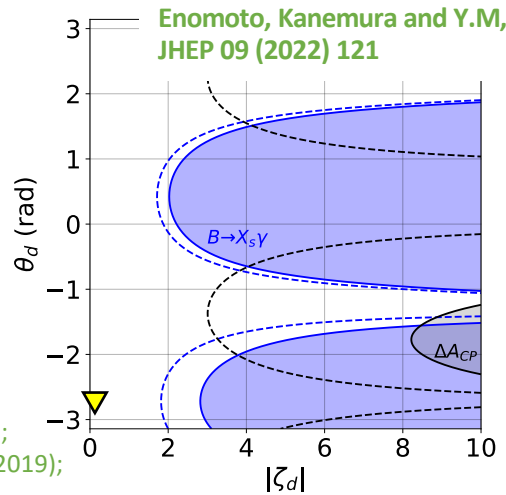
• Future flavor and EDM experiments for testing CPV

Blue : $B \rightarrow X_s \gamma$

Black :

$$\Delta A_{CP} = A_{CP}(B^+ \rightarrow X_s^+ \gamma) - A_{CP}(B^0 \rightarrow X_s^0 \gamma)$$

$$A_{CP}(X) \equiv \frac{\Gamma(\bar{X}) - \Gamma(X)}{\Gamma(\bar{X}) + \Gamma(X)}$$

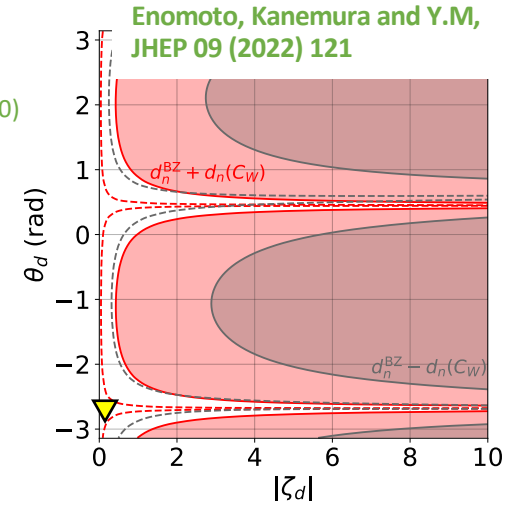


$$|d_n| < 1.8 \times 10^{-26} e \text{ cm}$$

Abel et al. [nEDM] (2020)

Red : $d_n + C_W$ case

Gray : $d_n - C_W$ case

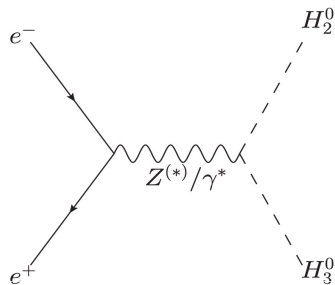


Benzke et al. Phys. Rev. Lett. 106 (2011);
Watanuki et al. [Belle] Phys. Rev. D 99 (2019);

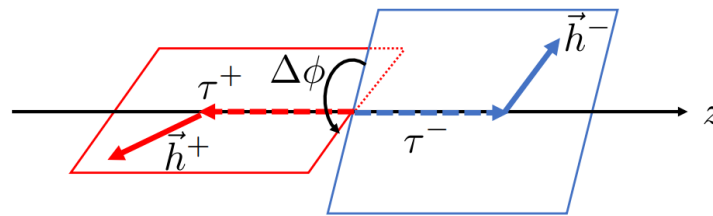
• CPV in the decays of the neutral scalar bosons ($|\zeta_d| \ll |\zeta_e|$ case)

Phase of ζ_e would be measured at upgraded ILC

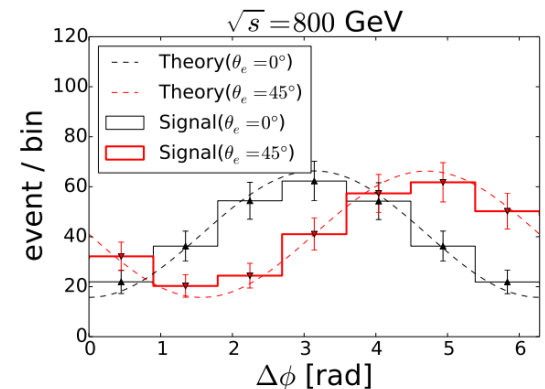
Kanemura, Kubota and Yagyu, JHEP 04 (2021) 144



$$H_{2,3} \rightarrow \tau^+ \tau^- \rightarrow X^+ \bar{\nu} X^- \nu$$



Jeans and Wilson, Phys. Rev. D 98 (2018) 013007



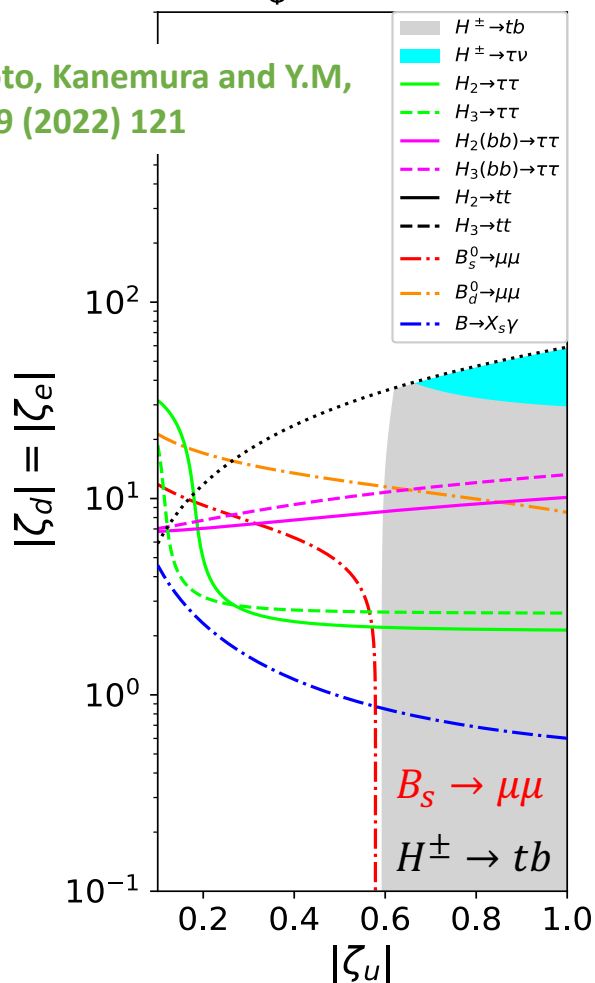
Many channels to test our scenario

$$m_\Phi \equiv m_{H_2} = m_{H_3} = m_{H^\pm}$$

- Multi lepton search at (HL-) LHC

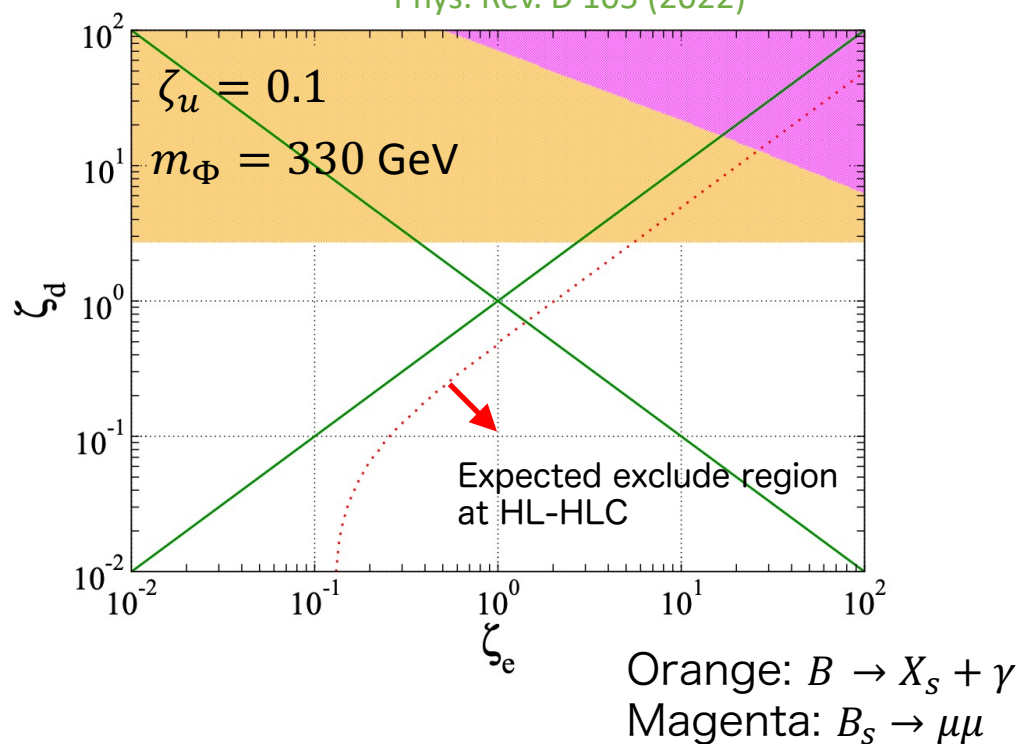
$m_\Phi = 350$ GeV

Enomoto, Kanemura and Y.M,
JHEP 09 (2022) 121



$pp \rightarrow \Phi\Phi \rightarrow$ multi leptons

Kanemura, Takeuchi and Yagyu
Phys. Rev. D 105 (2022)



Top-charm mixing EWBG

- General structure of Yukawa interaction

h SM Higgs
 $H_{2,3}$ Additional scalars

up-type quark

$$-\mathcal{L}_Y = \overline{u_{i,L}} \frac{y_i \delta_{ij}}{\sqrt{2}} u_{j,R} h - \overline{u_{i,L}} \frac{\rho_{ij}}{\sqrt{2}} u_{j,R} H_2 - \overline{u_{i,L}} \frac{i\rho_{ij}}{\sqrt{2}} u_{j,R} H_3 + \text{h.c.}$$

- Top-charm sector can be sizable under current data

Ex) $\rho_{tc} \lesssim O(1)$

- Consider FCNC couplings in top-charm sector

Top-charm transport scenario

S. Kanemura and Y.M, arXiv: 2303.11252

$$\rho^u = \begin{pmatrix} 0 & 0 & 0 \\ 0 & \rho_{cc} & \rho_{ct} \\ 0 & \rho_{tc} & \rho_{tt} \end{pmatrix}, \quad \rho^d = \begin{cases} \rho_{bb} & (i = j = 3) \\ 0 & (\text{others}) \end{cases} \quad \text{and} \quad \rho^e = 0$$

- Only $|\rho_{tc}|$ contributes to the BAU by picking up the effect of θ_7
- In previous studies, CPV phase of ρ_{tc} generates the BAU

Top-charm mixing

Fuyuto, Hou and Senaha, PLB 776 402 (2018)

Tau-mu mixing

Chiang, Fuyuto and Senaha, PLB 762 315 (2016)

CPV source with mixing in previous studies

- CPV interaction to the bubble walls

Top-charm mixing

Fuyuto, Hou and Senaha, PLB 776 402 (2018)

Contributions of 2nd generation was not included

- Source of top in weak basis

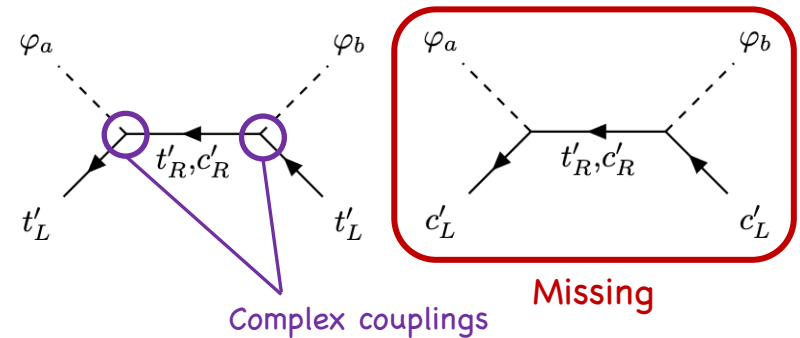
$$-\mathcal{L}_y \supset \overline{u'_{i,L}} (Y_{1,ij} \phi_1^{0*} + Y_{2,ij} \phi_2^{0*}) u'_{j,R},$$

$$S_{t'_L} \propto \text{Im}[Y_{1tt} Y_{2tt}^* + Y_{1tc} Y_{2tc}^*] = \text{Im}[(Y_1 Y_2^\dagger)_{tt}]$$

$$= \text{Im}[\underline{(V_L^\dagger Y_{\text{diag}} \rho^\dagger V_L)}_{tt}]$$

cause phase dependence of ρ_{tc}

Primed means weak basis



- Take into account “charm” contribution, which is defined in weak basis

$$S_{t'_L} + S_{c'_L} \propto \text{Im}[(Y_1 Y_2^\dagger)_{cc} + (Y_1 Y_2^\dagger)_{tt}]$$

$$= \text{Im}[\text{Tr}(Y_1 Y_2^\dagger)] = \text{Im}[\text{Tr}(Y_{\text{diag}} \rho^\dagger)] = -y_c \text{Im}[\rho_{cc}] - y_t \text{Im}[\rho_{tt}],$$

- ρ_{tc} does not contribute to BAU, unless consider CPV potential

Top-charm transport scenario

- **Benchmark point (wall velocity = 0.1)**

Related to...

phase transition and BAU

$$m_\Phi \equiv m_{H_2} = m_{H_3} = m_{H^\pm} = 350 \text{ GeV}, M = 20 \text{ GeV},$$

$$\lambda_2 = 0.01, |\lambda_7| = 1.0, \arg(\lambda_7) = -2.4, |\rho_{tt}| = 0.1, \theta_{tt} = -0.2,$$

constraints and predictions

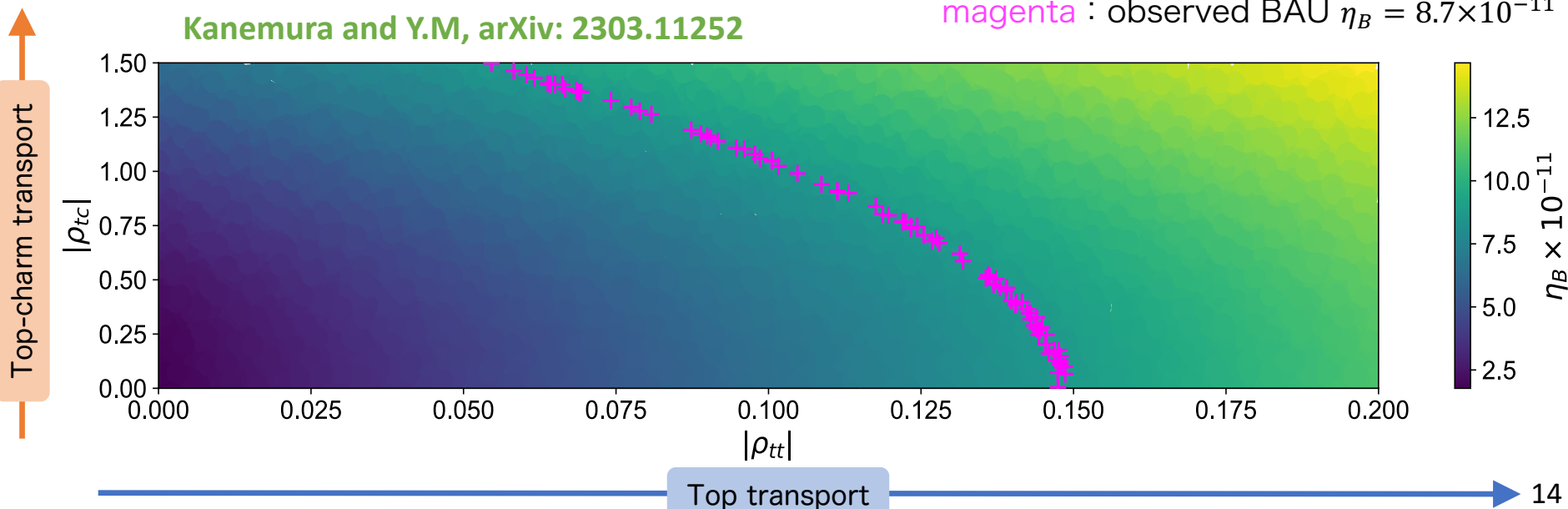
$$|\rho_{cc}| = 0.09, |\rho_{ct}| = 0.05, \theta_{cc} = 0, \theta_{ct} = -2.8, \theta_{tc} = -0.2,$$

$$|\rho_{bb}| = 1.0 \times 10^{-3}, \theta_{bb} = 1.5.$$

- **Impact of ρ_{tc} coupling to the BAU**

Kanemura and Y.M, arXiv: 2303.11252

magenta : observed BAU $\eta_B = 8.7 \times 10^{-11}$



Top-charm transport scenario

• Flavor constraints on FCNC couplings

Green : $B_s \rightarrow \mu\mu$ CMS (2022)

Others : $B_d - \bar{B}_d, B_s - \bar{B}_s$ mixing and $B \rightarrow X_s \gamma$

Gray : ϵ_K ($K^0 - \bar{K}^0$ mixing)

UTfit (2018), J. Haller et.al. (2018) and HFLAV (2022)

Chen and Nomur (2018)

• Predictions for future Kaon physics

Blue : $\Delta R_V^+ = \text{Br}(K^+ \rightarrow \pi^+ \nu \bar{\nu}) / \text{Br}(K^+ \rightarrow \pi^+ \nu \bar{\nu})_{\text{SM}} - 1$ [%]

Iguro and Omura (2019)

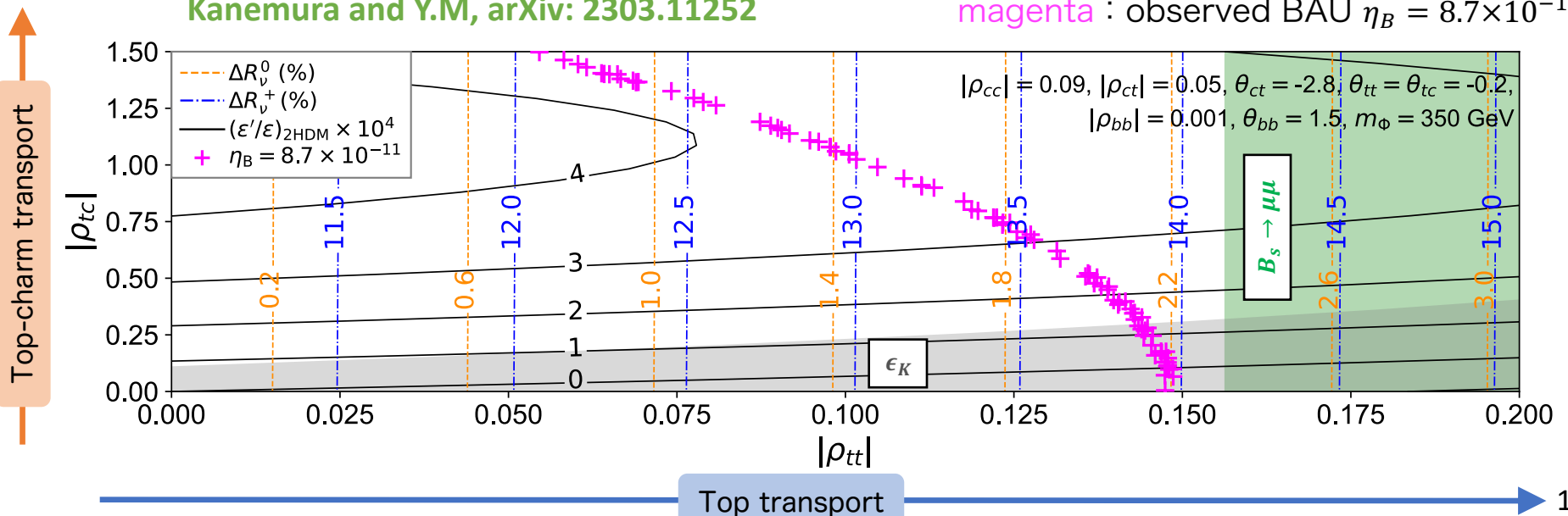
Orange : $\Delta R_V^0 = \text{Br}(K_L \rightarrow \pi^0 \nu \bar{\nu}) / \text{Br}(K_L \rightarrow \pi^0 \nu \bar{\nu})_{\text{SM}} - 1$ [%]

Hou and Kumar (2022)

Black : $(\epsilon' / \epsilon)_{2\text{HDM}} \times 10^4$

Kanemura and Y.M, arXiv: 2303.11252

magenta : observed BAU $\eta_B = 8.7 \times 10^{-11}$



Summary

- ◆ **SM cannot explain the Baryon Asymmetry of the Universe**

 - EWBG as a solution of the BAU is well motivated scenario

- ◆ **Viable EWBG scenario under current experimental data**

 - Two Higgs doublet model with alignment scenario
 - Multiple CP phases in the model
 - Difficulty from EDM constraints can be avoided

- ◆ **Phenomenology**

 - Common testability
 - Higgs self coupling (ILC, CLIC, HL-LHC)
 - Gravitational waves (LISA, DECIGO, BBO)
 - EDM, Direct detection and Flavor experiments (B meson physics)
 - Top-charm transport scenario → Kaon physics becomes important

Back up slides

About top-charm

Source term with top-charm mixing

- Two flavor fermions system

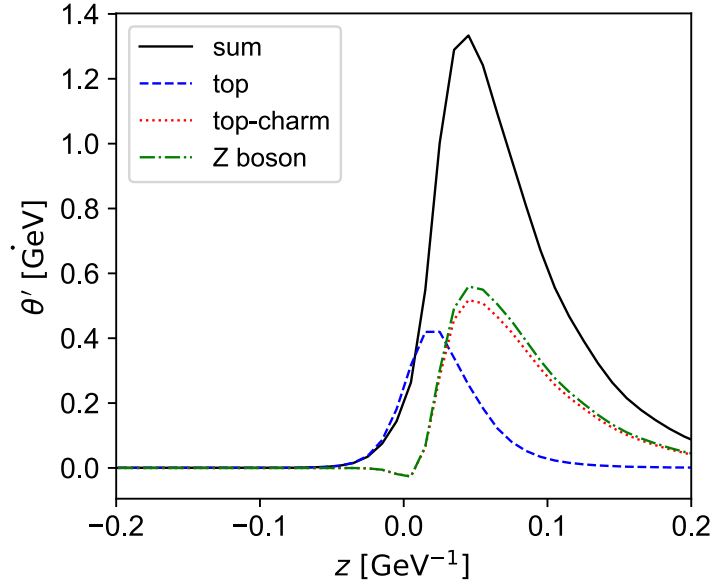
$$\mathcal{L}_{\text{mass}} = -\overline{q}_L M(z) q_R + \text{h.c.}, \quad q = (c, t)^T$$

$$M(z) = \frac{1}{\sqrt{2}} \begin{pmatrix} y_c \varphi_1 + \rho_{cc}(\varphi_2 - i\varphi_3) & \rho_{ct}(\varphi_2 - i\varphi_3) \\ \rho_{tc}(\varphi_2 - i\varphi_3) & y_t \varphi_1 + \rho_{tt}(\varphi_2 - i\varphi_3) \end{pmatrix}$$

φ_1 : Real part of $\langle \Phi_1^0 \rangle$, φ_2 : Real part of $\langle \Phi_2^0 \rangle$,
 φ_3 : Imaginary part of $\langle \Phi_2^0 \rangle$,

- WKB method

Cline, Joyce and Kainulainen, JHEP 07 (2000);
 Cline and Kainulainen, Phys. Rev. D 101 (2020)



- $\text{Abs}[\rho_{tc}]$ contributes to source term picking up CPV phase of the potential.

$$\theta' = \frac{1}{2m_+^2} \left\{ (|\rho_{tc}|^2 + |\rho_{tt}|^2)(\varphi_3\varphi_2' - \varphi_2\varphi_3') + y_t|\rho_{tt}| \left((\varphi_3\varphi_1' - \varphi_1\varphi_3') \cos \theta_{tt} + (\varphi_1\varphi_2' - \varphi_2\varphi_1') \sin \theta_{tt} \right) \right\} \\ + \frac{1}{\varphi_1^2 + \varphi_2^2 + \varphi_3^2} (\varphi_3\varphi_2' - \varphi_2\varphi_3') + O(\delta^2), \quad m_+ : \text{Local mass of heavy fermion}$$

- Contribution of $\text{arg}[\rho_{tc}]$ is negligibly small (below ~0.4%).

$$|M_{11}|/|M_{22}| \simeq |M_{12}|/|M_{22}| \equiv \delta \lesssim 0.06$$

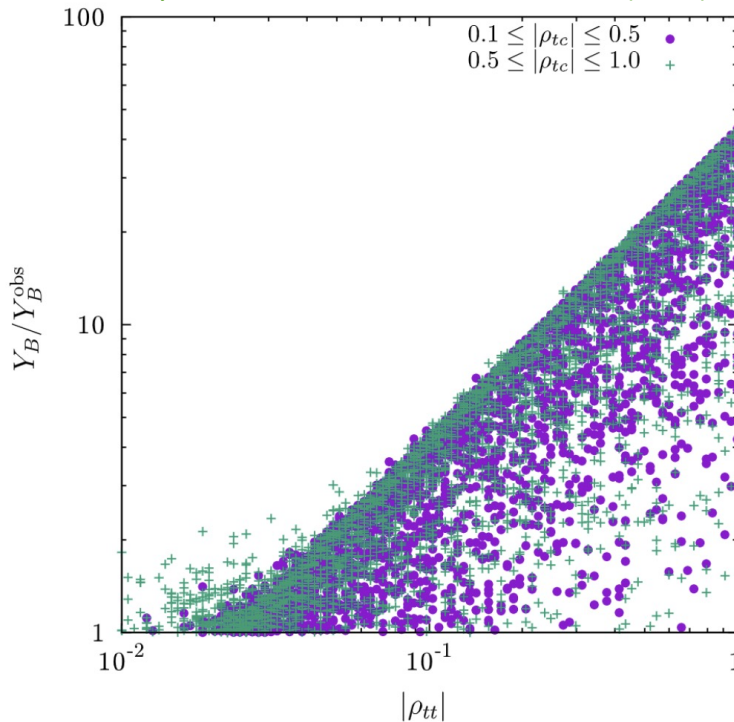
Inconsistent with Fuyuto, Hou and Senaha, PLB 776 402 (2018)
 given by VEV insertion approximation (VIA) 19

Previous results

- Both results are under CP conserving VEVs $\varphi_1, \varphi_2 \in \mathbb{R}$.

Top-charm mixing

Fuyuto, Hou and Senaha, PLB 776 402 (2018)



Tau-mu mixing

Chiang, Fuyuto and Senaha, PLB 762 315 (2016)

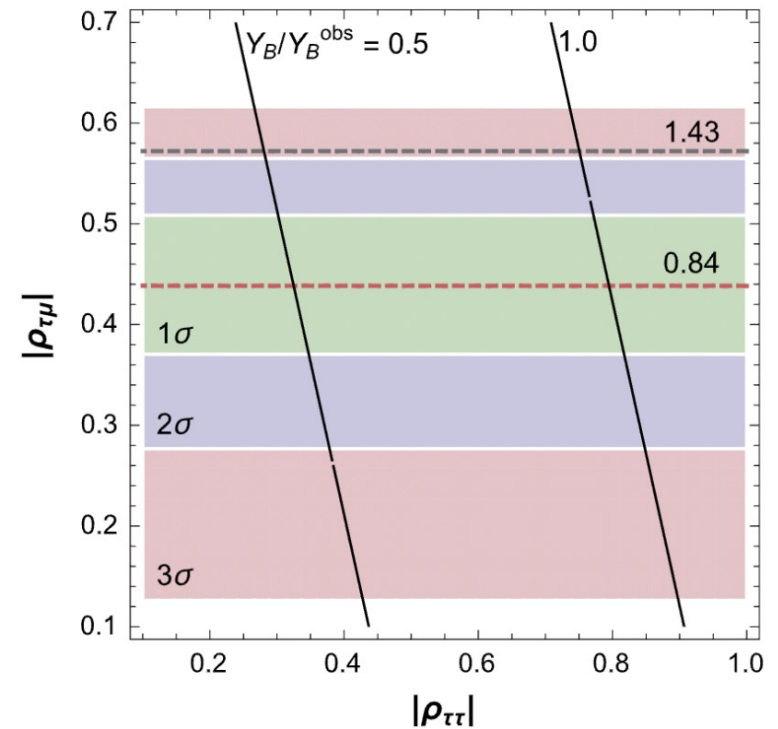


Fig. 2. Impact of ρ_{tt} and ρ_{tc} on Y_B , where the phases ϕ_{tt} and ϕ_{tc} are scanned over 0 to 2π , with other parameters randomly chosen (see text for details). The purple (green) points are for $0.1 \leq |\rho_{tc}| \leq 0.5$ ($0.5 \leq |\rho_{tc}| \leq 1.0$).

Fig. 2. Contours of Y_B/Y_B^{obs} , $\text{Br}(h \rightarrow \mu\tau)$ and δa_μ in the $(|\rho_{\tau\tau}|, |\rho_{\tau\mu}|)$ plane. We set $m_H = 350$ GeV, $m_A = m_{H^\pm} = 400$ GeV, $M = 100$ GeV, $c_{\beta-\alpha} = 0.006$, $|\rho_{\tau\mu}| = |\rho_{\mu\tau}|$, $\phi_{\tau\mu} = -5\pi/4$, $\phi_{\mu\tau} = \pi/4 - \phi_{\tau\mu}$ and $\phi_{\tau\tau} = \pi/2$. (For interpretation of the references to color in this figure, the reader is referred to the web version of this article.)

VIA source terms

- Boltzmann equation for fermion with field theoretical approach [A. Riotto \(1995\), \(1997\), \(1998\)](#)

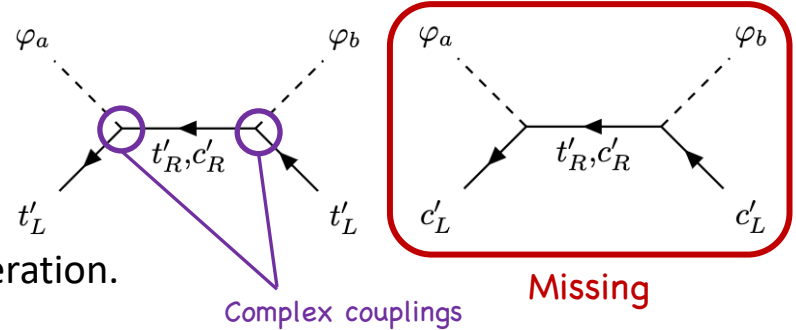
$$\partial_\mu^X j_\psi^\mu = - \int d^3\mathbf{w} \int_{-\infty}^T dw^0 \text{Tr} \left[\Sigma_\psi^>(X, w) G_\psi^<(w, X) - \Sigma_\psi^<(X, w) G_\psi^>(w, X) \right. \\ \left. - G_\psi^>(X, w) \Sigma_\psi^<(w, X) + G_\psi^<(X, w) \Sigma_\psi^>(w, X) \right],$$

- CP violations are included in self energy

Prime means weak basis

[Fuyuto, Hou and Senaha, PLB 776 402 \(2018\)](#)

does not contain contribution of 2nd generation.



- As [Fuyuto, Hou and Senaha](#), assuming CP conserving VEVs $\varphi_1, \varphi_2 \in \mathbb{R}$

Source of top in weak basis $-\mathcal{L}_y \supset \overline{u'_{i,L}} (Y_{1,ij} \phi_1^{0*} + Y_{2,ij} \phi_2^{0*}) u'_{j,R}$,

$$V_L(Y_1 + Y_2)V_R^\dagger = \sqrt{2}Y_{\text{diag}},$$

$$V_L(-Y_1 + Y_2)V_R^\dagger = \sqrt{2}\rho,$$

$$S_{t'_L} \propto \text{Im}[Y_{1tt}Y_{2tt}^* + Y_{1tc}Y_{2tc}^*] = \text{Im}[(Y_1Y_2^\dagger)_{tt}] = \text{Im}[(V_L^\dagger Y_{\text{diag}} \rho^\dagger V_L)_{tt}]$$

- Consider charm contribution in weak basis

$$S_{t'_L} + S_{c'_L} \propto \text{Im}[(Y_1Y_2^\dagger)_{cc} + (Y_1Y_2^\dagger)_{tt}]$$

$$= \text{Im}[\text{Tr}(Y_1Y_2^\dagger)] = \text{Im}[\text{Tr}(Y_{\text{diag}}\rho^\dagger)] = -y_c \text{Im}[\rho_{cc}] - y_t \text{Im}[\rho_{tt}],$$

Grossman-Nir bound

Grossman and Nir, PLB 398 163 (1997)

- Mixed Kaon states $|K_{L,S}\rangle = p|K^0\rangle \mp q|\bar{K}^0\rangle$
 - Define amplitudes $A = \langle \pi^0 \nu\nu | H | K^0 \rangle$, $\bar{A} = \langle \pi^0 \nu\nu | H | \bar{K}^0 \rangle$ and $\lambda = \frac{q}{p} \frac{\bar{A}}{A}$.
 - From measurement, $|q/p| \simeq 1$ and $|\lambda| \simeq 1$. $\pi^0 \sim (\bar{u}u - \bar{d}d)/\sqrt{2}$, $\pi^+ \sim \bar{d}u$,
 $K^0 \sim \bar{s}d$, $K^+ \sim \bar{s}u$
 - Using isospin symmetry relation $A(K^0 \rightarrow \pi^0 \nu\nu) = \frac{1}{\sqrt{2}} A(K^+ \rightarrow \pi^+ \nu\nu)$,
- we can find $\frac{\Gamma(K_L \rightarrow \pi^0 \nu\nu)}{\Gamma(K^+ \rightarrow \pi^+ \nu\nu)} \simeq \sin^2 \theta$, where $\lambda = e^{2i\theta}$.

- We obtain upper bound

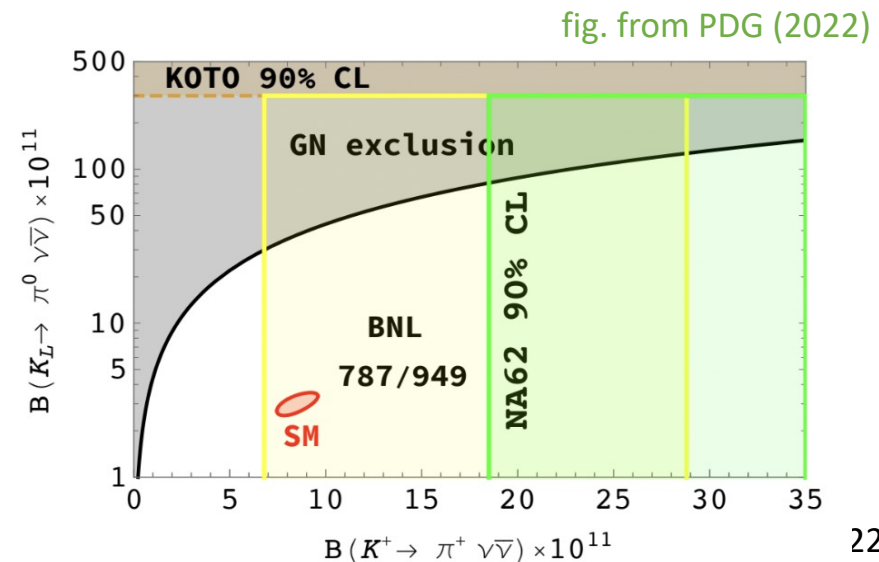
$$\text{Br}(K_L \rightarrow \pi^0 \nu\nu) \lesssim 4 \times \text{Br}(K^+ \rightarrow \pi^+ \nu\nu)$$

with $\tau_{K_L}/\tau_{K^+} \simeq 4.2$.

- SM predictions [J. Buras et.al. JHEP 11 \(2015\) 033](#)

$$\text{Br}(K^+ \rightarrow \pi^+ \nu\nu)_{\text{SM}} = (8.4 \pm 1.0) \times 10^{-11}$$

$$\text{Br}(K_L \rightarrow \pi^0 \nu\nu)_{\text{SM}} = (3.4 \pm 0.6) \times 10^{-11}$$



Direct CP violation in Kaon decay

- K_L (K_S) coincides with CP-odd (CP-even) state if CP is conserved.

✗ $K_L \rightarrow 2\pi$
 ○ $K_S \rightarrow 2\pi$

- Mixed Kaon states $|K_{L,S}\rangle = p |K^0\rangle \mp q |\bar{K}^0\rangle$

I : Isospin of two pion system

$$\epsilon' \equiv \frac{\langle I=2 | T | K_L \rangle \langle I=0 | T | K_S \rangle - \langle I=2 | T | K_S \rangle \langle I=0 | T | K_L \rangle}{\sqrt{2} \langle I=0 | T | K_S \rangle^2}$$

$$\propto \langle I=2 | T | K^0 \rangle \langle I=0 | T | \bar{K}^0 \rangle - \langle I=2 | T | \bar{K}^0 \rangle \langle I=0 | T | K^0 \rangle$$

rephasing invariant quantity
 represent direct CP violation

$$\frac{\epsilon'}{\epsilon} = -\frac{\omega}{\sqrt{2}|\epsilon_K|} \left[\frac{\text{Im}A_0}{\text{Re}A_0} (1 - \Omega_{\text{eff}}) - \frac{1}{a} \frac{\text{Im}A_2}{\text{Re}A_2} \right]$$

a, Ω_{eff} : Isospin breaking effects
 $\omega = \langle 2 | T | K^0 \rangle / \langle 0 | T | K^0 \rangle$

$$\frac{\epsilon'}{\epsilon} = \left(\frac{\epsilon'}{\epsilon} \right)_{\text{SM}} + \left(\frac{\epsilon'}{\epsilon} \right)_{\text{NP}},$$

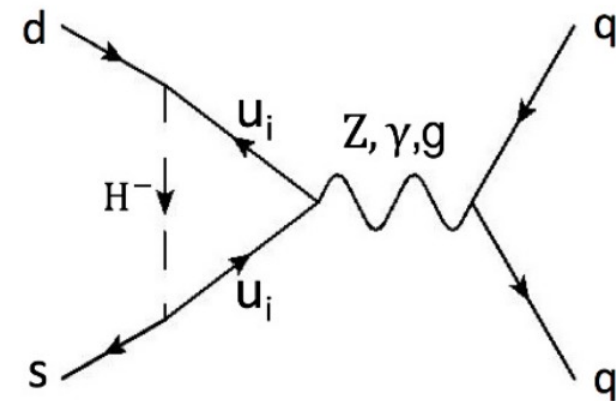
$$\left(\frac{\epsilon'}{\epsilon} \right)_{\text{NP}} \simeq \frac{G_F \omega}{2|\epsilon_K| \text{Re}A_0} \times \sum_{i,j} \langle Q_i(\mu) \rangle U_{ij}(\mu, \mu_{\text{NP}}) \text{Im} s_i(\mu_{\text{NP}}),$$

Kitahara, Nierste and Tremper (2016)

- Hadronic matrix elements with lattice results

$$\left(\frac{\epsilon'}{\epsilon} \right)_{\text{SM}} = (21.7 \pm 8.4) \times 10^{-4}$$

Blum et. al. (2015), Abbott et. al. (2020)



This operator also causes $K \rightarrow \pi \nu \nu$ decays.

Collider constraints

- The most stringent constraints to ρ_{tc}

$$cg \rightarrow tH_2/H_3 \rightarrow tt\bar{c}$$

Same sign multi lepton signal

CMS, Eur. Phys. J. C 78 140 (2018)

CMS, Eur. Phys. J. C 80 75 (2020)

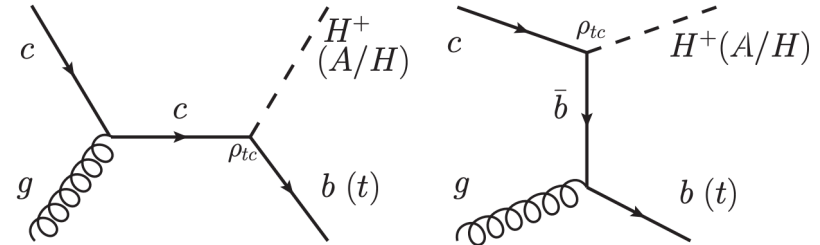


Fig. from Hou, Modak and Plehn (2021)

- Due to interference b/w $cg \rightarrow tH_2 \rightarrow ttc$ and $cg \rightarrow tH_3 \rightarrow ttc$, total cross section vanishes with $m_{H_2} = m_{H_3}$ and $\Gamma_{H_2} = \Gamma_{H_3}$.

Kohda, Modak, and Hou, Phys. Lett. B 776 379 (2018)

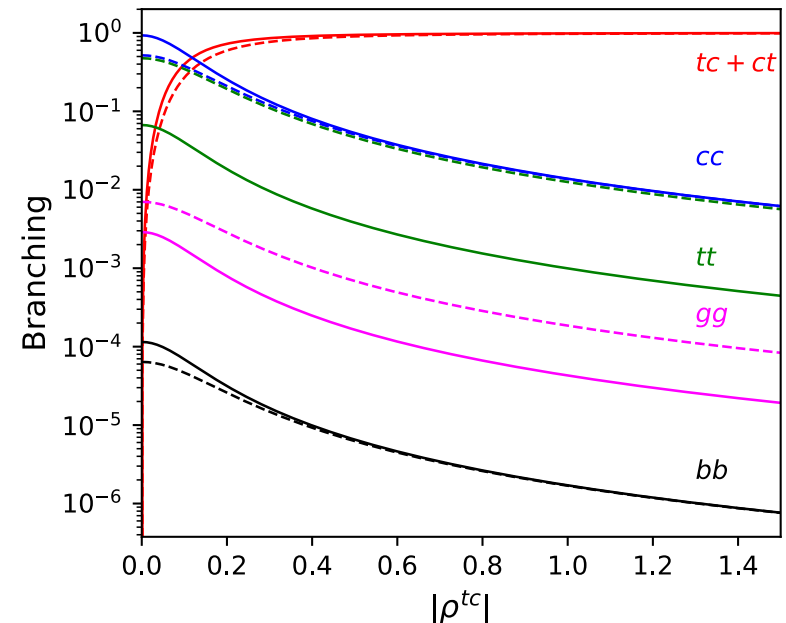
Kohda, Modak, and Hou, Phys. Lett. B 786 212 (2018)

- Difference of widths is small as $O(0.1)$ GeV, so that cross section is efficiently small.

Solid : H_2

Dashed : H_3

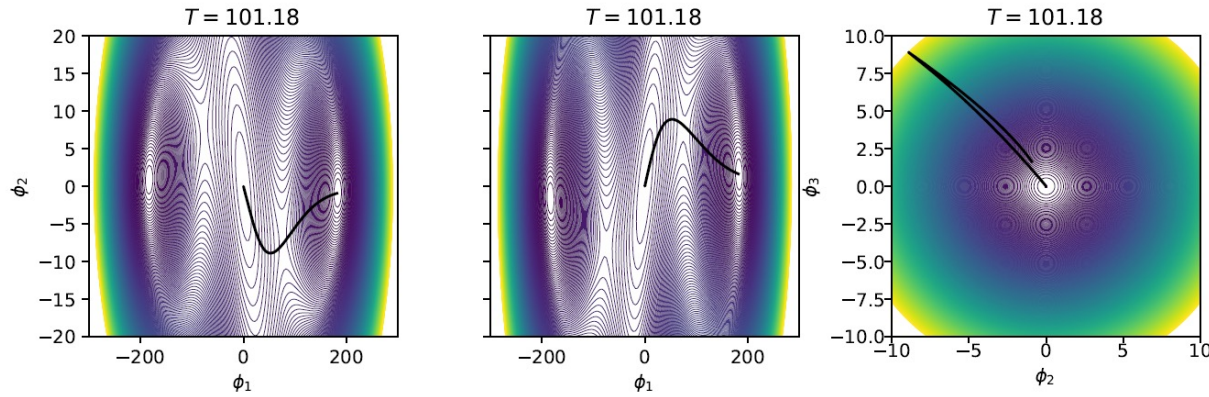
- Other collider constraints relevant to ρ_{tt} are weakened by large ρ_{tc} .



About BAU (top transport)

CP violating bubble

Order parameter $h_1 = h, h_2 = H \cos \varphi_H, h_3 = H \sin \varphi_H$



Black line is the path of PT.

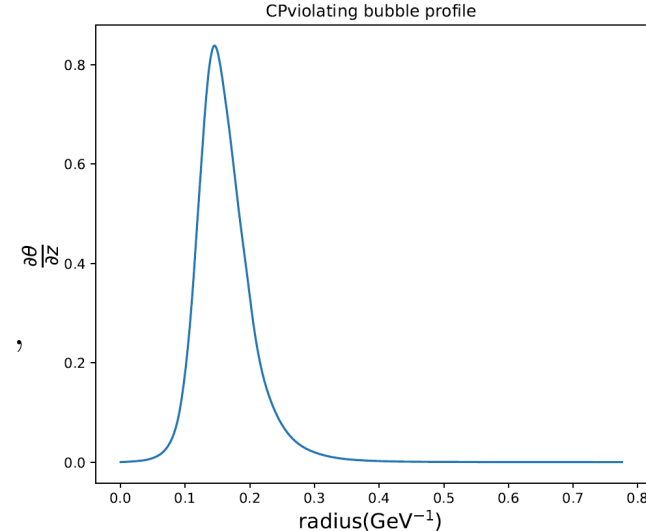
Vertical: Heavy scalar mode
Horizontal: Light scalar mode

Large VEVs $\phi_{2,3}$ during PT are needed for BAU.

Localized top phase

$$\partial_z \theta(z) = -\frac{\varphi_H^2}{\varphi_{H_1}^2 + \varphi_H^2} \partial_z \theta_H - \partial_z \arctan \left(\frac{|\zeta_u| \varphi_H \sin(\theta_H + \theta_u)}{\varphi_{H_1} + |\zeta_u| \varphi_H \cos(\theta_H + \theta_u)} \right),$$

$$\varphi_H \equiv \sqrt{\varphi_{H_2}^2 + \varphi_{H_3}^2}, \quad \theta_H = \arctan(\varphi_{H_2}/\varphi_{H_3}),$$



We used CosmoTransitions to calculate the bubble wall profile.

Wainwright, Comput. Phys. Commun. 183 (2011)

Estimation of baryon density

Top transport scenario Fromme and Huber, JHEP 03 (2007)

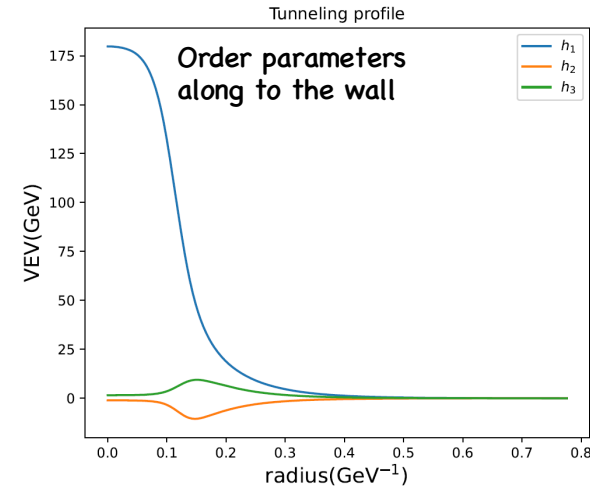
CP violating source is the top quark which has large yukawa coupling.

Localized top quark mass

$$m_t(z) = \frac{y_t}{\sqrt{2}} v(z) e^{i\theta(z)}$$

Higgs potential at finite temperature determines the bubble profile.

v(z), \theta(z), T_n, L_w, ...



“Semi classical force mechanism” (WKB method)

Cline, Joyce and Kainulainen, JHEP 07 (2000);
Cline and Kainulainen Phys. Rev. D 101 (2020)

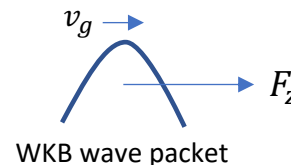
Boltzmann equation

$$(\partial_t + \mathbf{v}_g \cdot \partial_x + \mathbf{F} \cdot \partial_p) f_i = C[f_i, f_j, \dots]$$

$$v_g = \frac{p_z}{E_0} \left(1 \pm s \frac{\theta'}{2} \frac{m^2}{E_0^2 E_{0z}} \right)$$

$$F_z = -\frac{(m^2)'}{2E_0} \pm s \frac{(m^2 \theta')'}{2E_0 E_{0z}} \mp s \frac{\theta' m^2 (m^2)'}{4E_0^3 E_{0z}}$$

Overall signs are flipped between particles and anti-particles.



Particle distributions are small away from its equilibrium form

$$f_i = \frac{1}{e^{\beta[\gamma_w(E_i + v_w p_z) - \mu_i]} \pm 1} + \delta f_i$$

Transport equations

Boltzmann equation $(\partial_t + \mathbf{v}_g \cdot \partial_{\mathbf{x}} + \mathbf{F} \cdot \partial_{\mathbf{p}})f_i = C[f_i, f_j, \dots]$

$$v_g = \frac{p_z}{E_0} \left(1 \pm s \frac{\theta'}{2} \frac{m^2}{E_0^2 E_{0z}} \right)$$

$$F_z = -\frac{(m^2)'}{2E_0} \pm s \frac{(m^2\theta)'}{2E_0 E_{0z}} \mp s \frac{\theta' m^2 (m^2)'}{4E_0^3 E_{0z}}$$

Overall signs are flipped between particle and anti-particle.

Particle distributions are small away from its equilibrium form

$$f_i = \frac{1}{e^{\beta[\gamma_w(E_i + v_w p_z) - \mu_i]} \pm 1} + \delta f_i$$

Boltzmann equation can be expanded by small wall velocity, and after integrated in momentum,

$$v_w K_1 \mu' + v_w K_2 (m^2)' \mu + u' - \langle C[f] \rangle = 0 \quad (\text{K series are z-dependent functions})$$

$$-K_4 \mu' + v_w \tilde{K}_5 u' + v_w \tilde{K}_6 (m^2)' u - \left\langle \frac{p_z}{E_0} C[f] \right\rangle = S_\theta \quad S_\theta = -v_w K_8 (m^2 \theta)' + v_w K_9 \theta' m^2 (m^2)'$$

Plasma flame

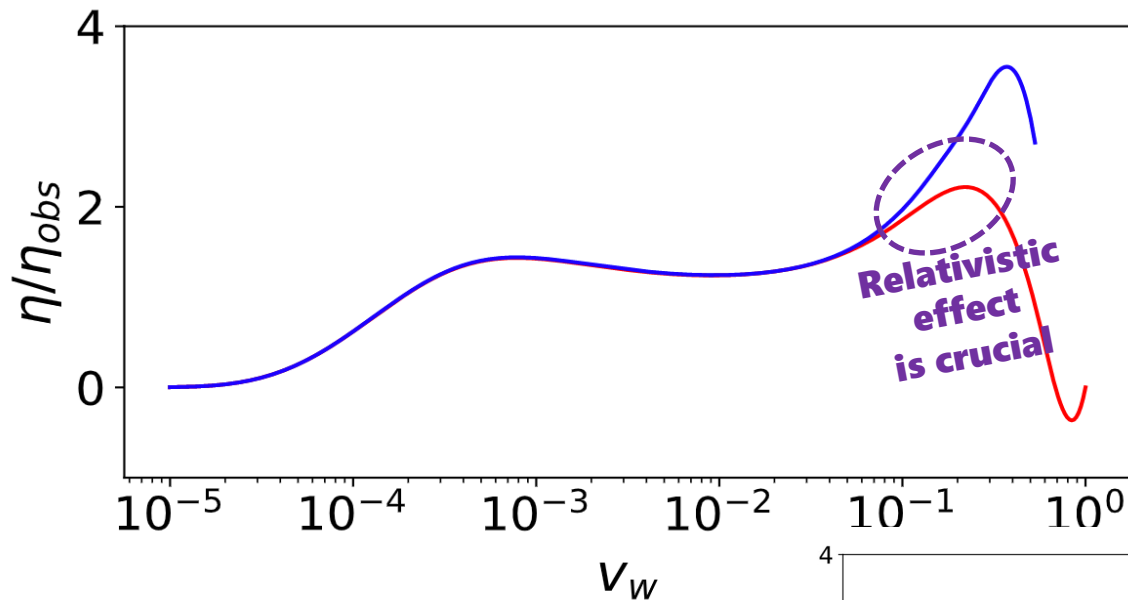
$$\frac{\partial n_B}{\partial t} = \frac{3}{2} \Gamma_{\text{sph}} \left(3\mu_{BL} - \frac{A}{T^3} n_B \right)$$

Integrated in wall flame

$$\eta_B = \frac{405 \Gamma_{\text{sph}}}{4\pi^2 v_w g_* T} \int_0^\infty dz \mu_{BL} f_{\text{sph}} e^{-45 \Gamma_{\text{sph}} z / (4v_w)}$$

$$f_{\text{sph}}(z) = \min \left(1, \frac{2.4T}{\Gamma_{\text{sph}}} e^{-40v(z)/T} \right)$$

Velocity dep. of baryon density

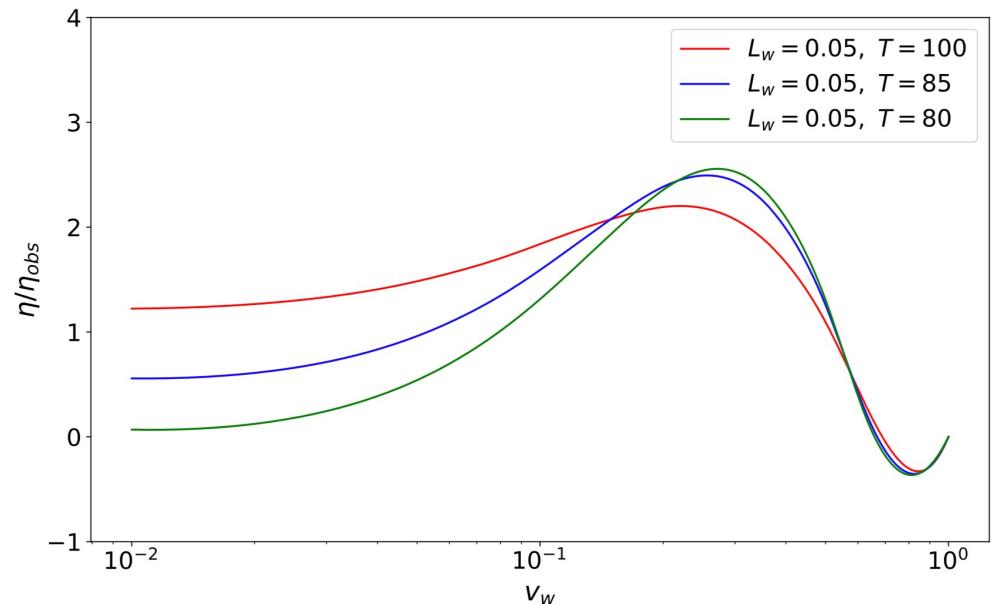


For the predictable GWs, relativistic effects must be included.

Blue: Fromme and Huber, JHEP 03 (2007)

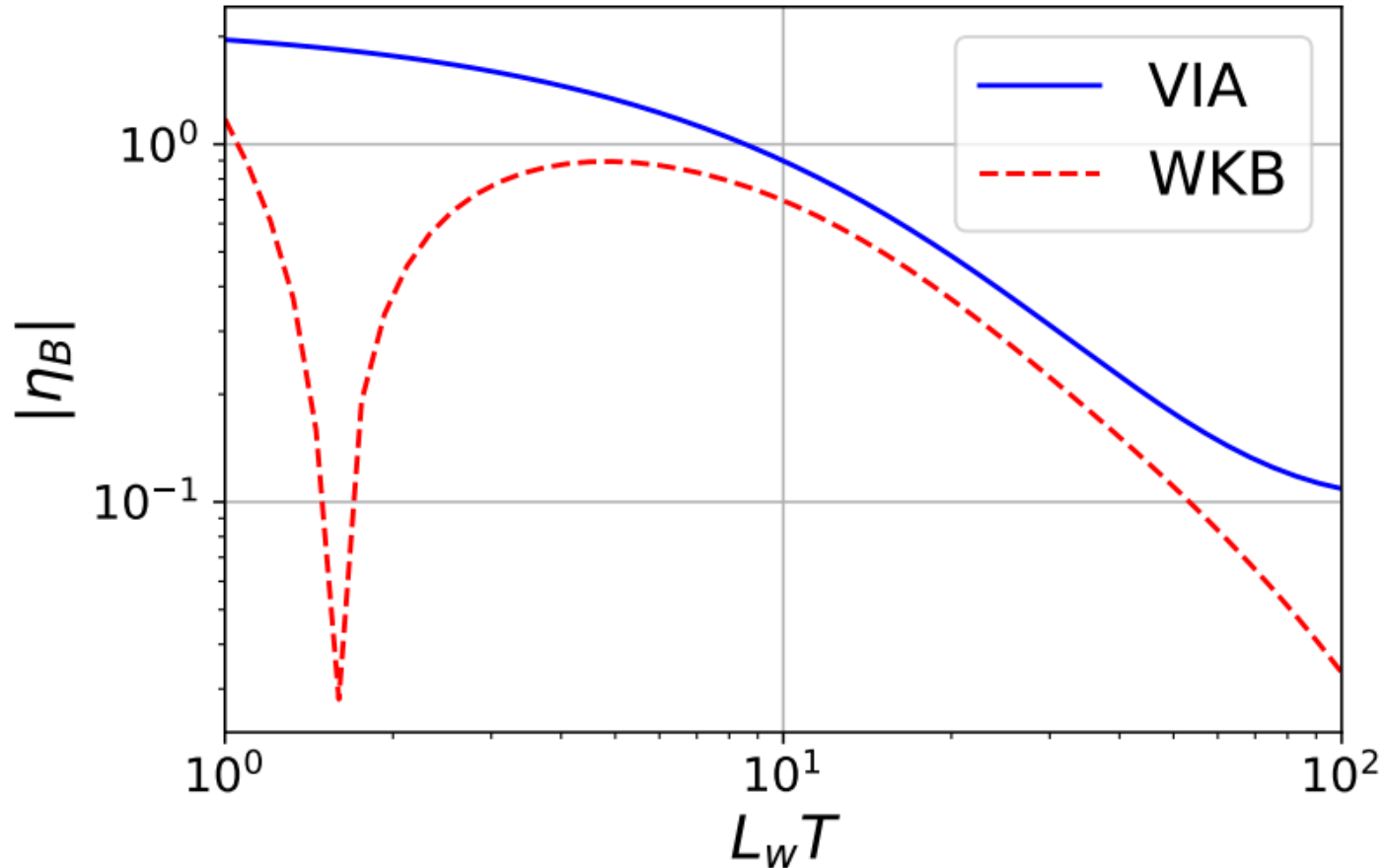
Red: Cline and Kainulainen, Phys. Rev. D 101 (2020)

Velocity dependences differ in nucleation temperatures.



Wall width dependence of BAU

Cline and Laurent, Phys. Rev. D 104 (2021)



WKB formalism has accidental zero-crossing behavior.

Supplement figures

Previous studies

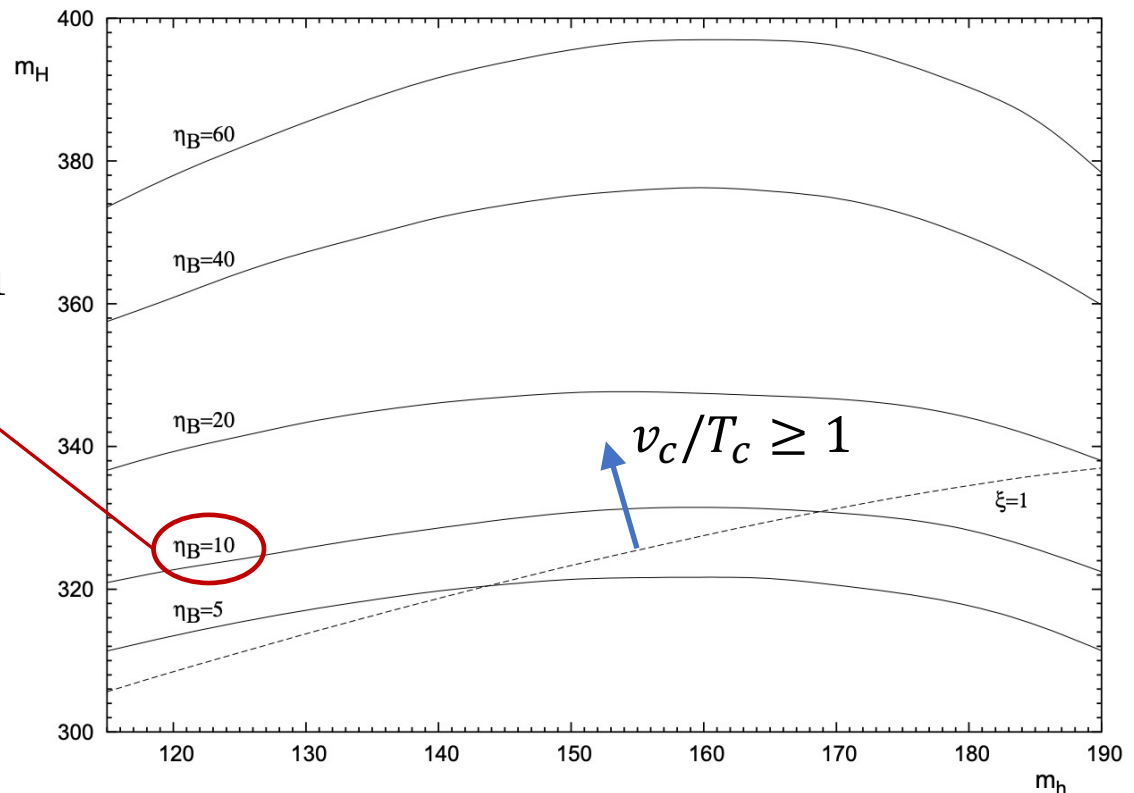
Fromme, Huber and Seniuchi, JHEP 11 (2006) 038

- Robust estimation of the BAU in two Higgs doublet model

$$V_0(\Phi_1, \Phi_2) = -\mu_1^2 \Phi_1^\dagger \Phi_1 - \mu_2^2 \Phi_2^\dagger \Phi_2 - \mu_3^2 (e^{i\alpha} \Phi_1^\dagger \Phi_2 + \text{h.c.}) \\ + \frac{\lambda_1}{2} (\Phi_1^\dagger \Phi_1)^2 + \frac{\lambda_2}{2} (\Phi_2^\dagger \Phi_2)^2 + \lambda_3 (\Phi_1^\dagger \Phi_1) (\Phi_2^\dagger \Phi_2) \\ + \lambda_4 |\Phi_1^\dagger \Phi_2|^2 + \frac{\lambda_5}{2} \left((\Phi_1^\dagger \Phi_2)^2 + \text{h.c.} \right)$$

Softly broken Z_2 symmetry
to avoid FCNC couplings

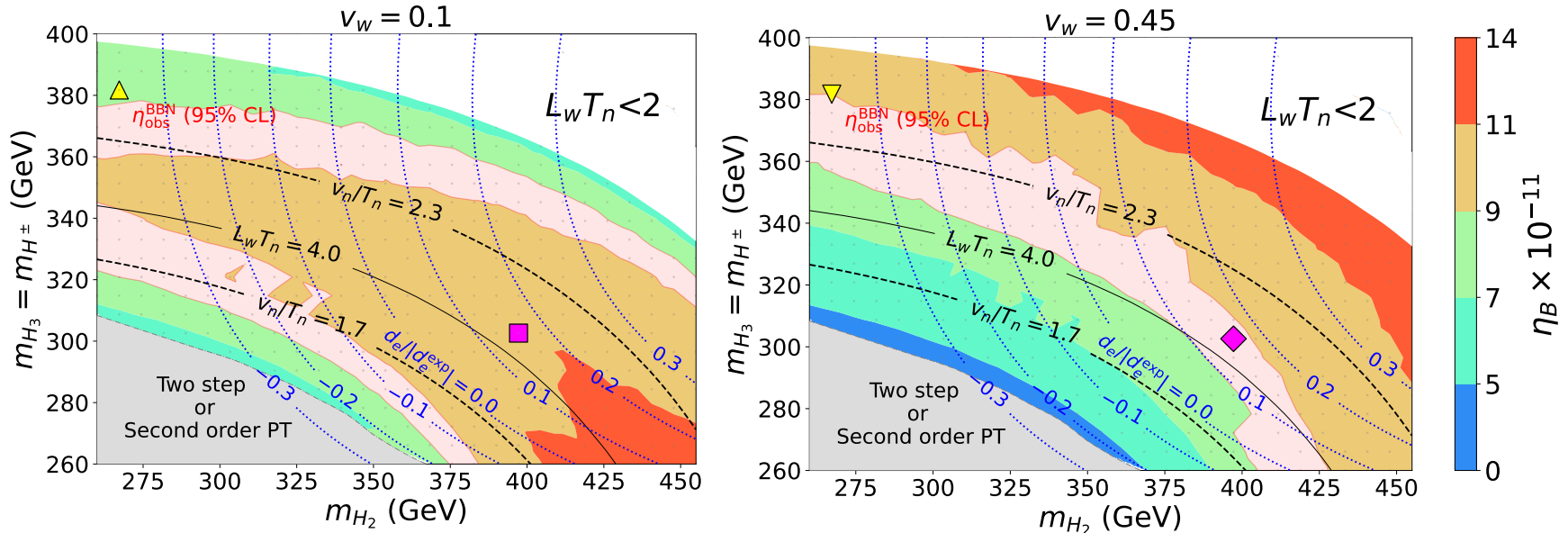
observed BAU: $\eta_B \simeq 10 \times 10^{-11}$



Velocity dependence of BAU

Baryon asymmetry in the relativistic bubble wall velocity Cline and Kainulainen, Phys. Rev. D 101 (2020)

Assuming the velocity as a free parameter



Strongly first order PT (except for gray region)

$$M = 30 \text{ GeV}, \quad \lambda_2 = 0.1, \quad |\lambda_7| = 0.8, \quad \theta_7 = -0.9,$$

The observed BAU (pink) $\eta_{obs}^{BBN} \equiv \frac{n_B}{s} = 8.2\text{--}9.2 \times 10^{-11}$ $|\zeta_u| = |\zeta_d| = |\zeta_e| = 0.18, \quad \theta_u = -2.7, \quad \delta_d = 0, \quad \delta_e = -0.04.$

Electron EDM (blue dotted)

$$|d_e^{exp}| < 1.1 \times 10^{-29} e \text{ cm}$$

Andreev et al. [ACME] Nature 562 (2018)

[green: relate to the BAU
blue: relate to the eEDM
purple: relate to the both

We set four benchmarks :

- ▲ BP1a: small velo. + strongly PT
- ▼ BP1b: large velo. + strongly PT
- BP2a: small velo. + weakly PT
- ◆ BP2b: large velo. + weakly PT

Effective potential

Thermal resummation → Parwani scheme

1 loop potential → Landau gauge ($\xi = 0$)

Renormalization condition

→ MS-bar scheme ($\lambda_{2,7}, M$) + On-shell scheme (other parameters)

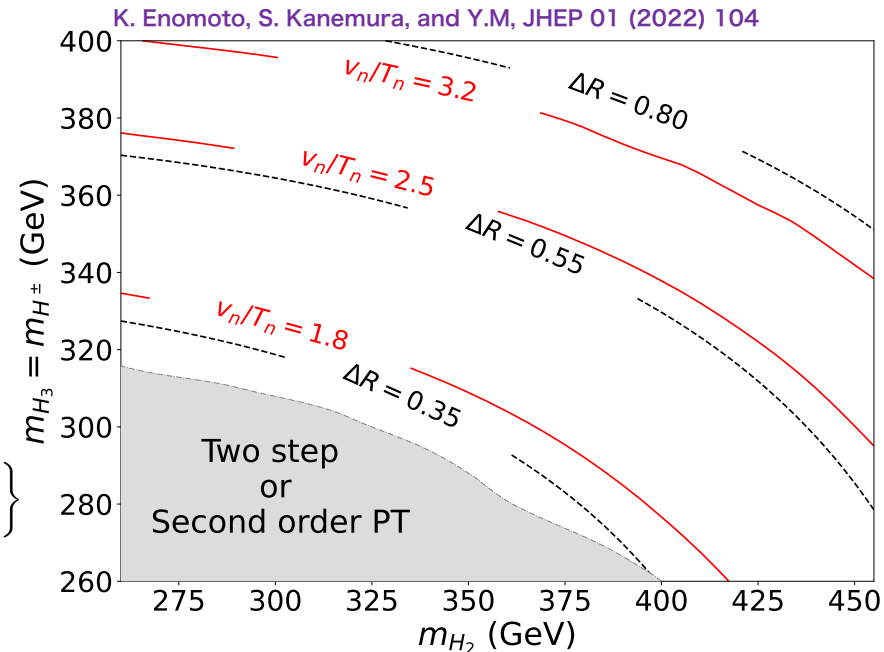
$$\left. \frac{\partial V}{\partial h_i} \right|_{\substack{h_1=v \\ h_2=h_3=0}} = 0 \quad \text{We used cutoff } m_{NG} = m_{IR} \sim 1 \text{ GeV to avoid IR divergence.}$$

$$\left. \frac{\partial^2 V}{\partial h_i \partial h_j} \right|_{\substack{h_1=v \\ h_2=h_3=0}} = \mathcal{M}_{ij}^2$$

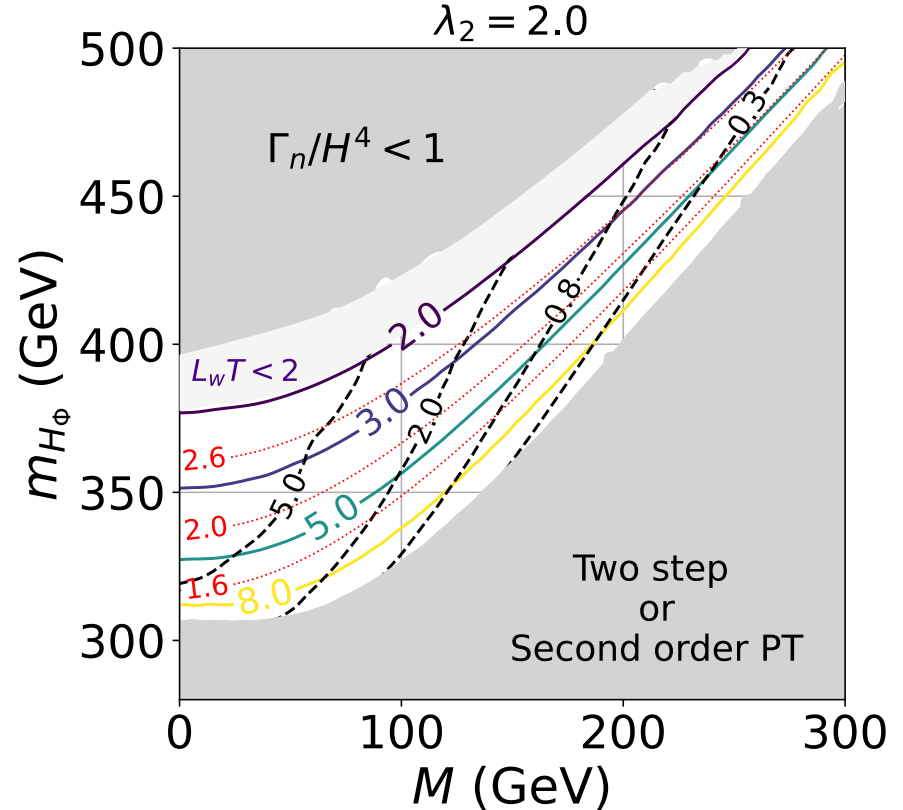
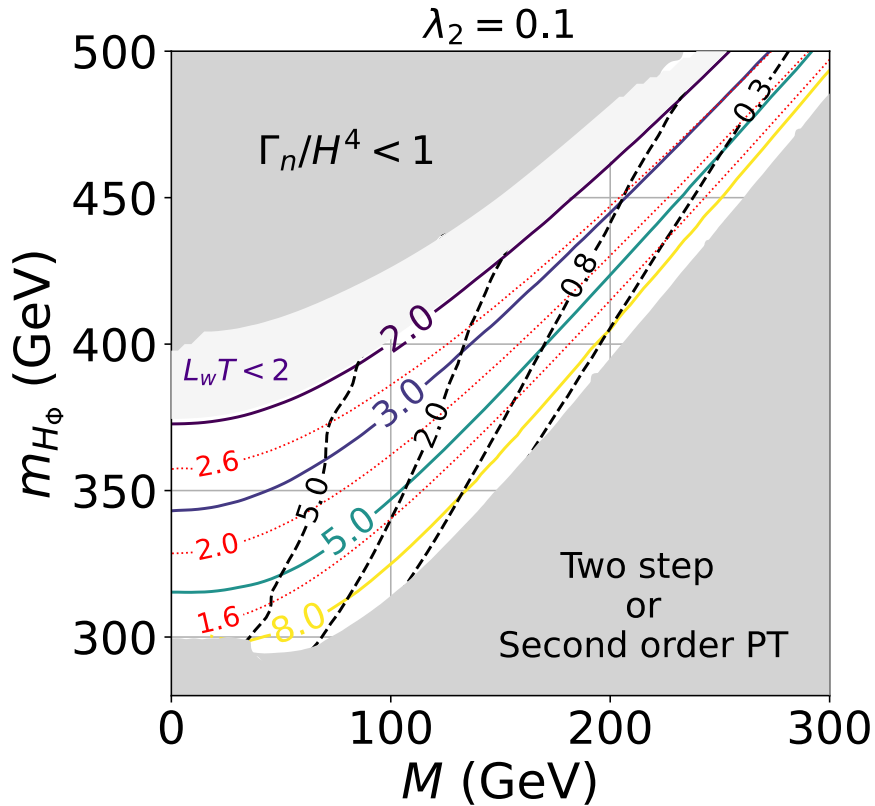
Higgs triple coupling at 1 loop level

$$\Delta R \equiv \frac{\lambda_{hhh} - \lambda_{hhh}^{\text{SM}}}{\lambda_{hhh}^{\text{SM}}} \simeq \frac{1}{12\pi^2 v^2 m_{H_1}^2} \left\{ 2 \frac{(m_{\pm}^2 - M^2)^3}{m_{\pm}^2} + \frac{(m_{H_2}^2 - M^2)^3}{m_{H_2}^2} + \frac{(m_{H_3}^2 - M^2)^3}{m_{H_3}^2} \right\}$$

Relation between ϕ/T and ΔR (right figure)



EW Phase transition



When M and λ_2 are large, $\partial_z \theta|_{max}$ becomes small.

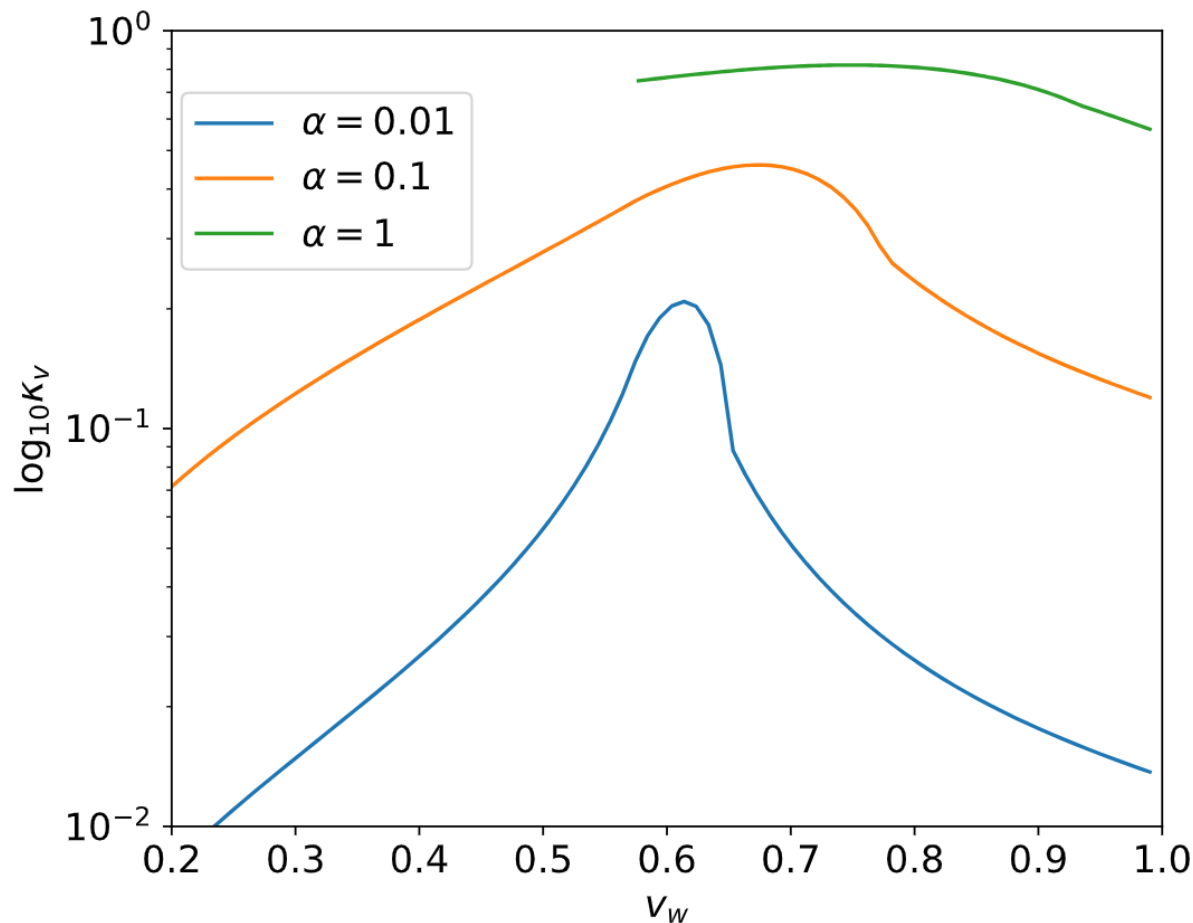
Source term $S_\theta = -v_w K_8 (m^2 \theta')' + v_w K_9 \theta' m^2 (m^2)'$

Red dotted : v_n/T_n
 Color solid : $L_w T$
 Black dashed : $\partial_z \theta|_{max}$

Velocity dep. of efficiency factor

Efficiency $\kappa_v(\alpha, v_w)$ means how much the latent heat is converted to the sound waves.

No hydrodynamical eq. exists when $\alpha \sim 1$, $v_w \lesssim c_s$. Espinosa *et al.* JCAP 06 (2010)



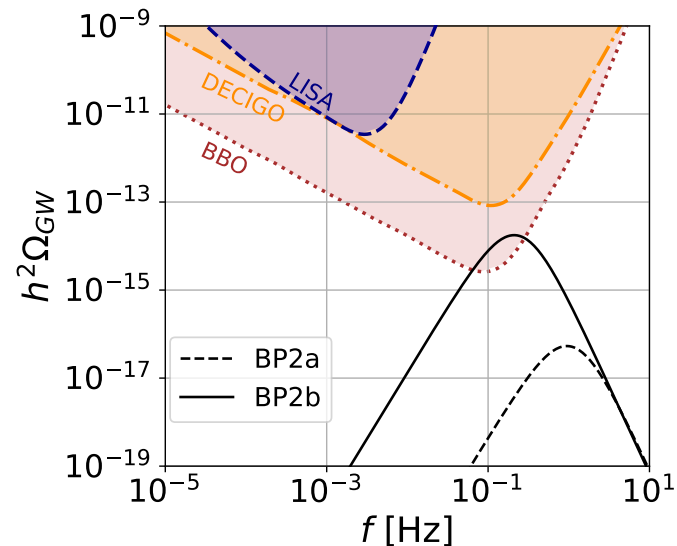
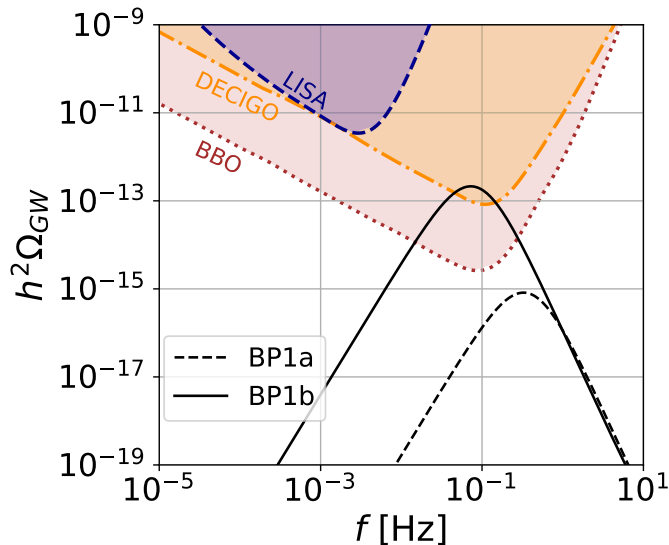
Gravitational waves from EWPT

		v_w	m_{H_2}	m_{H_3, H^\pm}	M	v_n/T_n	$L_w T_n$	η_B	ΔR	$\sigma \mathcal{B}(H_1 \rightarrow \gamma\gamma)$
Strongly PT	small velo. \blacktriangle	BP1a	267 GeV	381 GeV	30 GeV	2.4	2.6	7.8×10^{-11}	0.61	$104 \pm 5 \text{ fb}$
	large velo. \blacktriangledown	BP1b						9.1×10^{-11}		
Weakly PT	small velo. \blacksquare	BP2a	397 GeV	302 GeV	30 GeV	2.0	4.1	10.8×10^{-11}	0.44	
	large velo. \blacklozenge	BP2b						9.0×10^{-11}		

Gravitational wave spectra

Grojean and Servant, Phys. Rev. D 75 (2007);
Kakizaki, Kanemura and Matsui, Phys. Rev. D 92 (2015); and more

Sensitivity curves Hashino *et al.* Phys. Rev. D 99 (2019)



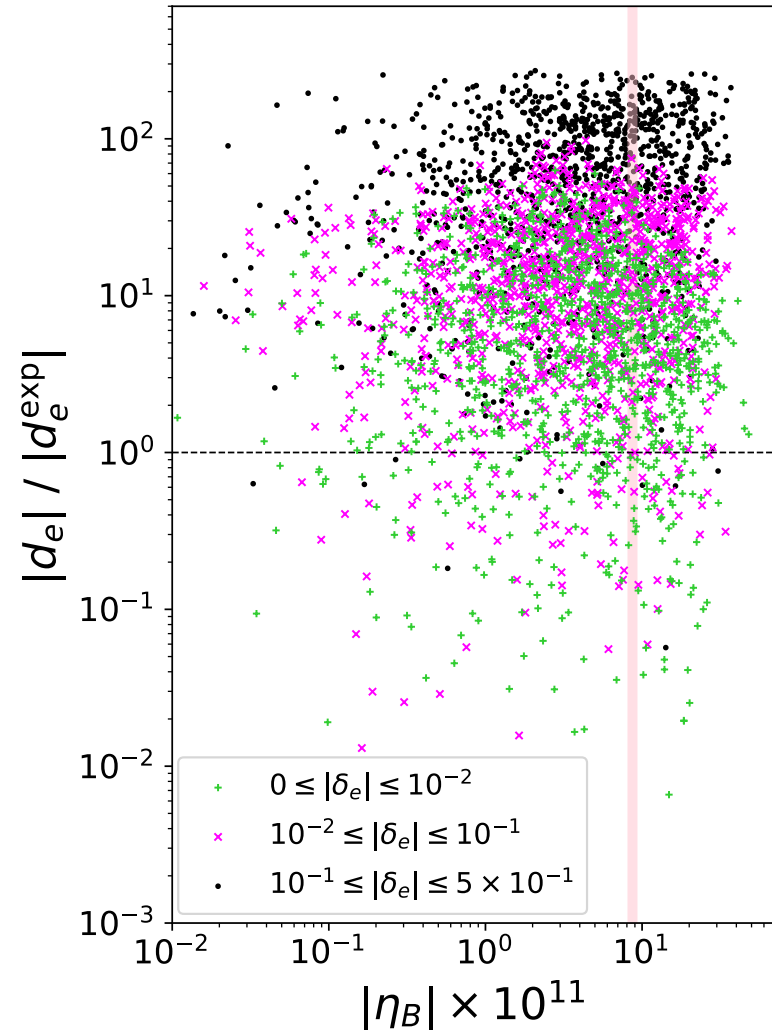
Strong PT and large velocity are needed.

BP1b and BP2b can also be tested by GW observation.

Scatter plot for eEDM and BAU

$$\lambda_2 = 0.1, m_{\Phi} = 350 \text{ GeV}, M = 30 \text{ GeV}, v_w = 0.1,$$

$$\theta_u = \theta_d = [0, 2\pi), |\zeta_d| = |\zeta_e| = [0, 10], |\lambda_7| = [0.5, 1.0], \theta_7 = [0, 2\pi).$$



These points are allowed from various constraints.

Fermion loop contributions

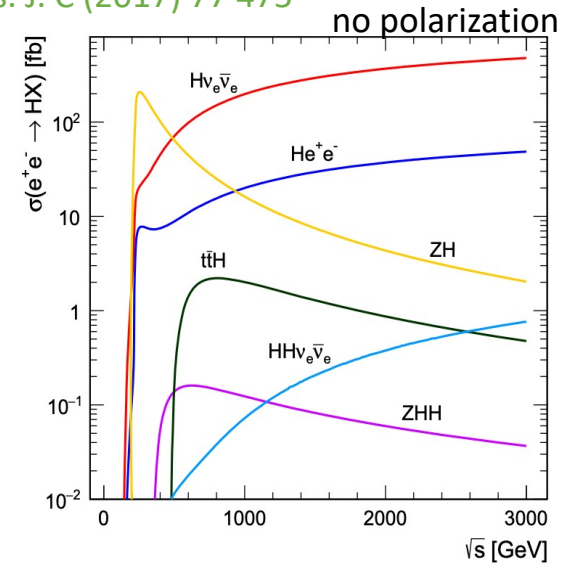
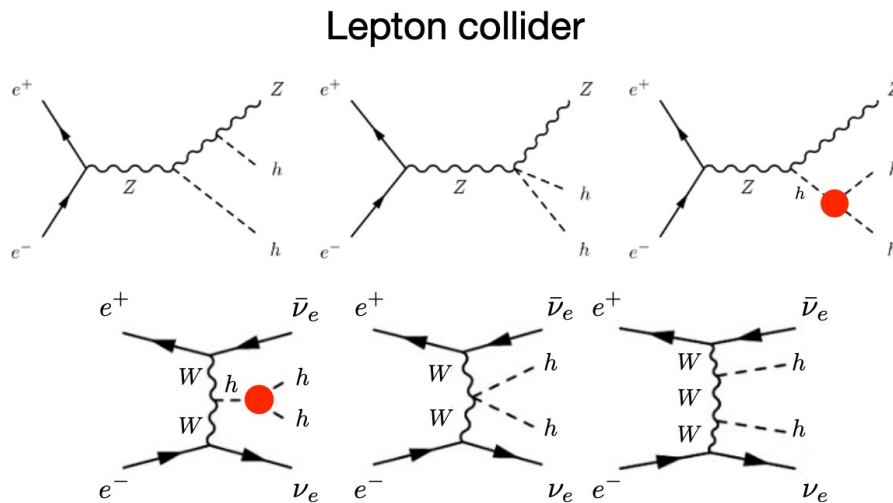
are proportional to $|\zeta_u||\zeta_e|\sin\delta_e$.

$$(\delta_e \equiv \theta_u - \theta_e)$$

Many points are satisfied from eEDM data
and they generate sufficient BAU.

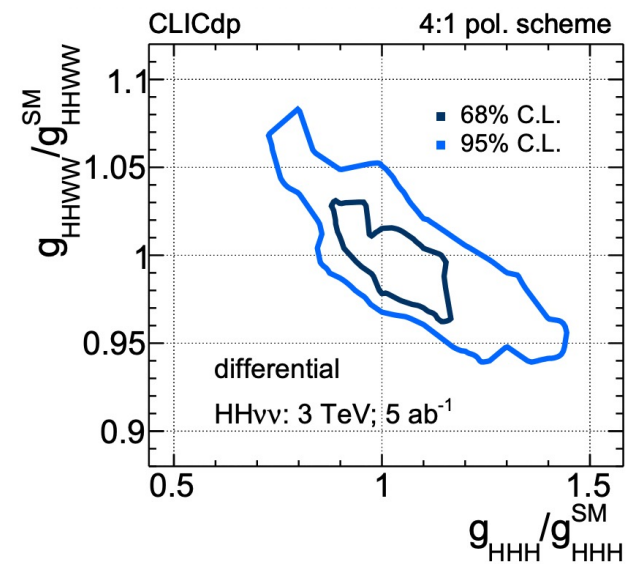
di-Higgs production at linear collider

Higgs production at e+ e- collider [Abramowicz et al., Eur. Phys. J. C \(2017\) 77 475](#)



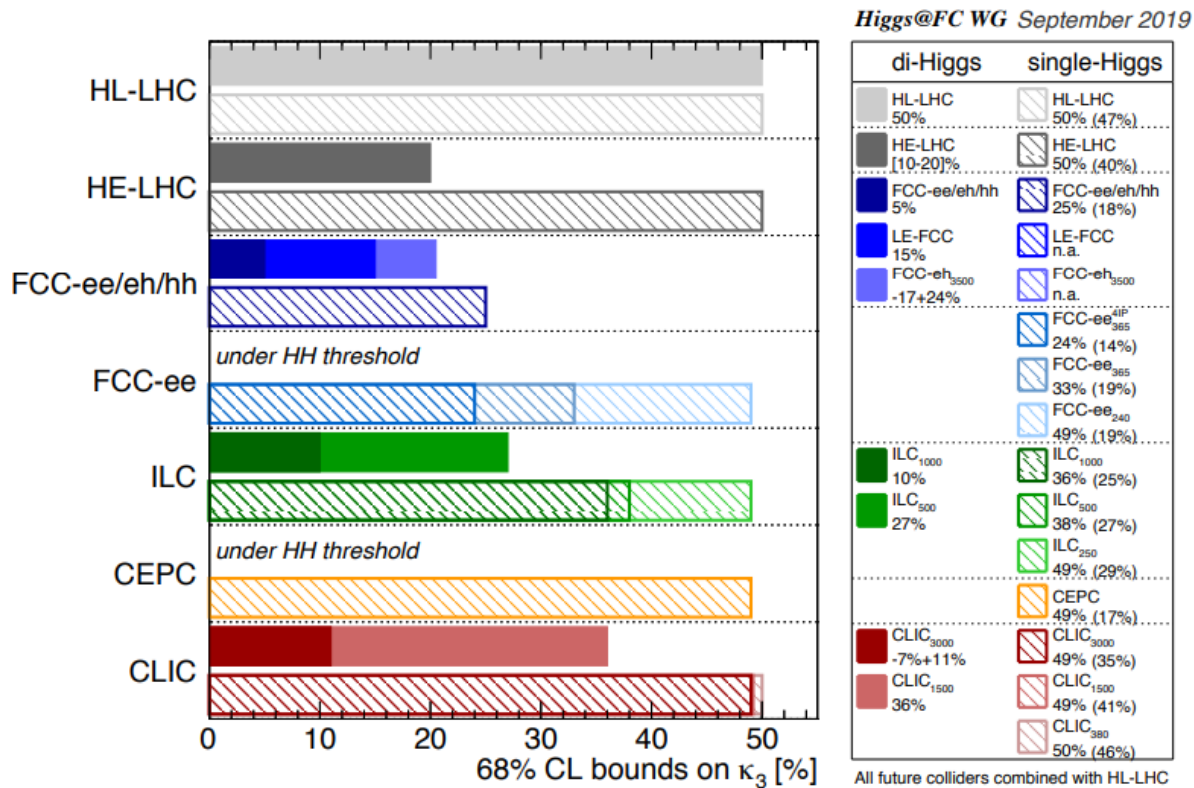
Higgs self coupling at CLIC Stage-3 (3 TeV)

[Philipp Roloff et al., Eur. Phys. J. C 80 \(2020\) 11, 1010](#)

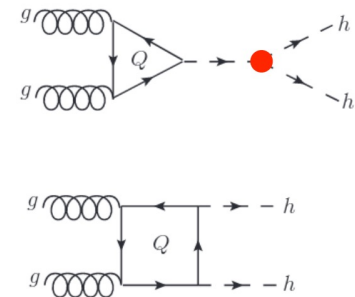


λ_{hhhh} measurement at future colliders

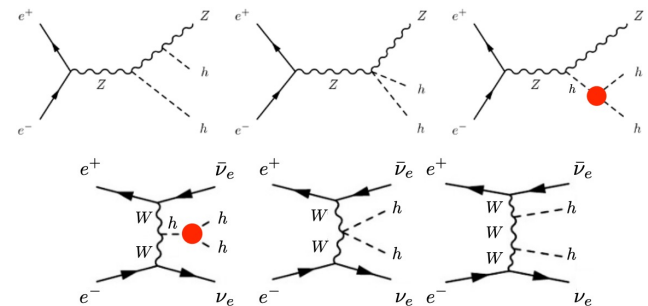
de Blas *et al.* JHEP 01(2020)



Hadron collider



Lepton collider



Testing CP violation

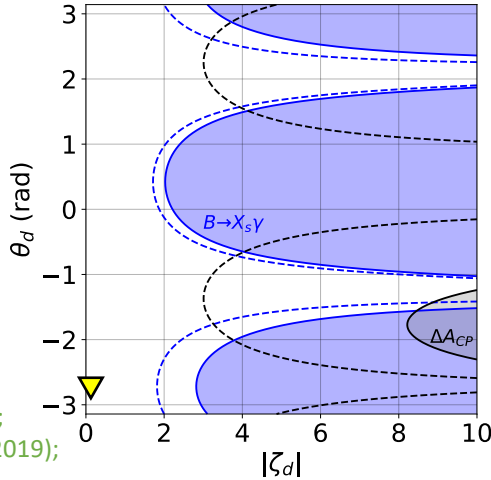
- Future flavor and EDM experiments for testing CPV

Blue : $B \rightarrow X_s \gamma$

Black :

$$\Delta A_{CP} = A_{CP}(B^+ \rightarrow X_s^+ \gamma) - A_{CP}(B^0 \rightarrow X_s^0 \gamma)$$

$$A_{CP}(X) \equiv \frac{\Gamma(\bar{X}) - \Gamma(X)}{\Gamma(\bar{X}) + \Gamma(X)}$$

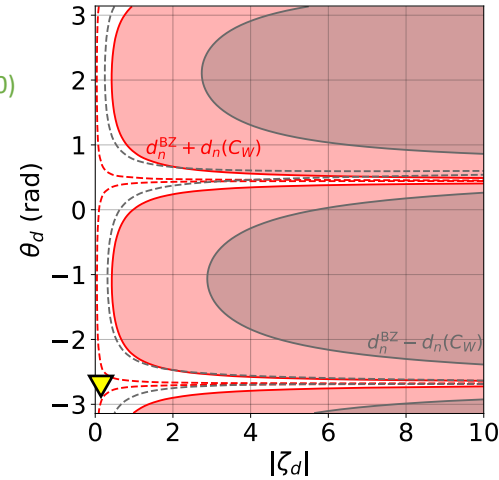


$$|d_n| < 1.8 \times 10^{-26} e \text{ cm}$$

Abel et al. [nEDM] (2020)

Red : $d_n + C_W$ case

Gray : $d_n - C_W$ case

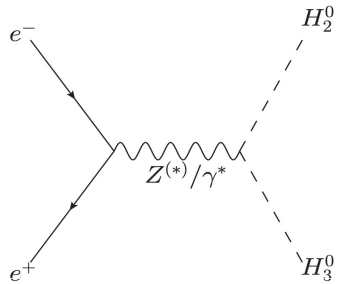


Benzke et al. Phys. Rev. Lett. 106 (2011);
Watanuki et al. [Belle] Phys. Rev. D 99 (2019);

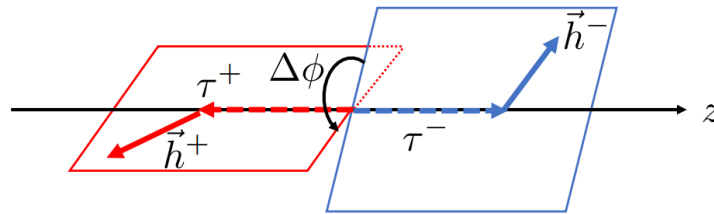
- CPV in the decays of the neutral scalar bosons ($|\zeta_d| \ll |\zeta_e|$ case)

Phase of ζ_e would be measured at upgraded ILC

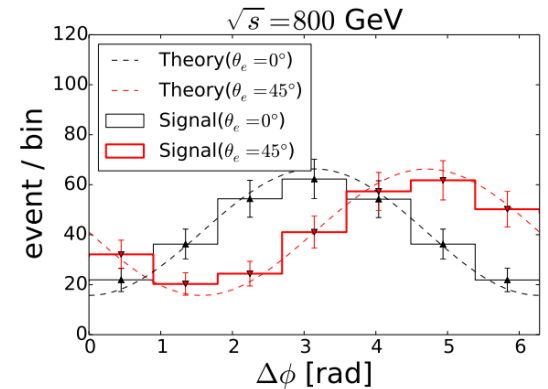
Kanemura, Kubota and Yagyu, JHEP 04 (2021) 144



$$H_{2,3} \rightarrow \tau^+ \tau^- \rightarrow X^+ \bar{\nu} X^- \nu$$



Jeans and Wilson, Phys. Rev. D 98 (2018) 013007



- Top-charm mixing effects on the BAU Kanemura and Y.M., arXiv:2303.11252

Constraints on the model

- Constraints from direct searches and various flavor observables

Direct search experiments

$H_{2,3} \rightarrow \tau\tau$ Aad *et al.* [ATLAS] Phys. Rev. Lett. 125 (2020)
 $H_{2,3}(bb) \rightarrow \tau\tau$
 $H_{2,3} \rightarrow tt$ Aaboud *et al.* [ATLAS] Eur. Phys. J. C 78 (2018);
 Sirunyan *et al.* [CMS] JHEP 04 (2020)
 $H^\pm \rightarrow tb$ Aad *et al.* [ATLAS] JHEP 06 (2021)
 $H^\pm \rightarrow \tau\nu$ Sirunyan *et al.* [CMS] JHEP 07 (2019)

Flavor experiments

$B_d \rightarrow \mu\mu$ Amhis *et al.* [HFLAV] Eur. Phys. J. C 81 (2021);
 Haller *et al.* Eur. Phys. J. C 78 (2018);
 $B_s \rightarrow \mu\mu$ Aaboud *et al.* [ATLAS] JHEP 04 (2019);
 Sirunyan *et al.* [CMS] JHEP 04 (2020);
 $B \rightarrow X_s \gamma$ Aaij. *et al.* [LHCb] Phys. Rev. D 105 (2022)

$$|\zeta_u| = |\zeta_d| = |\zeta_e| \text{ (Type I 2HDM)}$$

 Experimental upper bound $|\zeta_u| \lesssim 0.6$

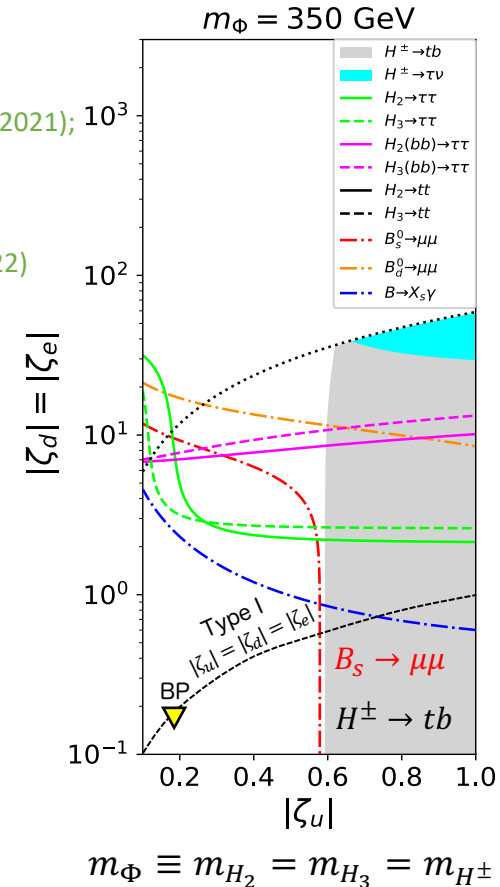
- Important Yukawa interaction for baryogenesis

$$\mathcal{L}_y \supset \zeta_u^* \frac{\sqrt{2}M_t}{v} \overline{Q_{3L}} \tilde{\Phi}_2 b_R + \text{h.c.},$$

Top transport scenario
 Fromme and Huber, JHEP 03 (2007) 049

- CPV interaction of top quarks to the bubble wall

Local mass term along to the bubble wall $m_t(z) = \frac{y_t}{\sqrt{2}} v(z) e^{i\theta(z)}$ generates BAU



Higgs to di-photon decay

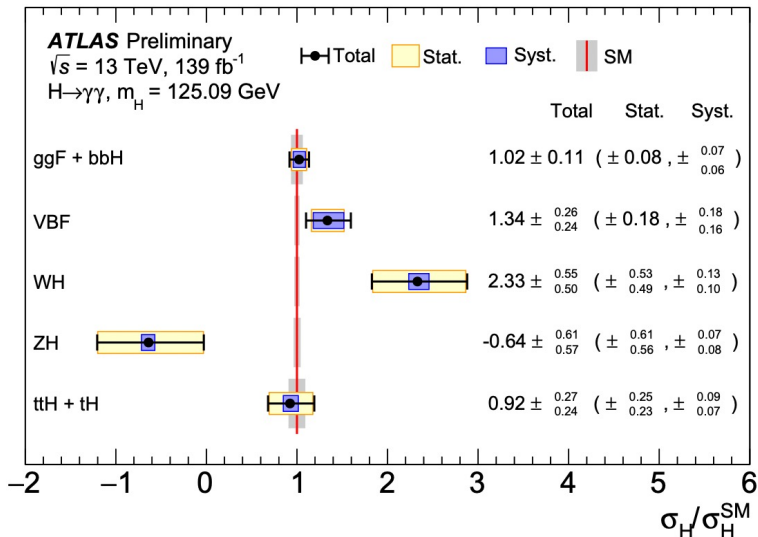
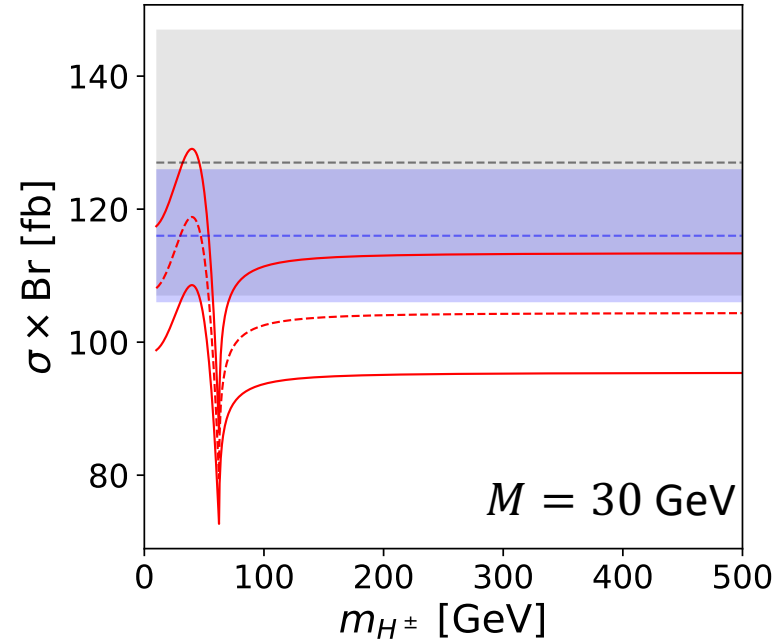
Non decoupling effect in $H_1 \rightarrow \gamma\gamma$

The constraints on the coupling $H_1 H^\pm H^\pm$

$$m_{H^\pm}^2 = M^2 + \frac{1}{2} \lambda_3 v^2$$

Red line is prediction in the case of $M = 30$ GeV.

SM expected (blue): $\sigma Br(H_1 \rightarrow \gamma\gamma) = 116 \pm 5$ fb



Observed (gray): $\sigma Br(H_1 \rightarrow \gamma\gamma) = 127 \pm 10$ fb

σ is inclusive production cross section of H_1 .

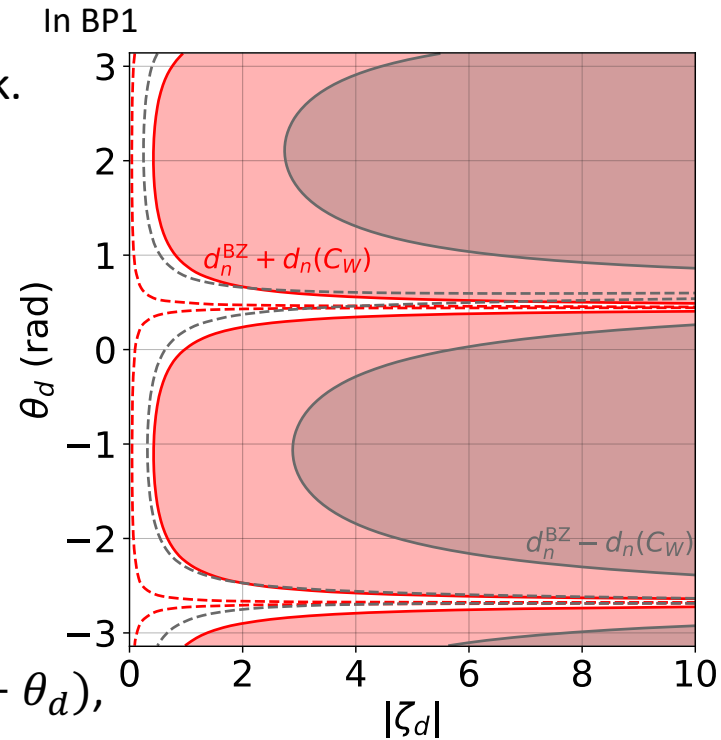
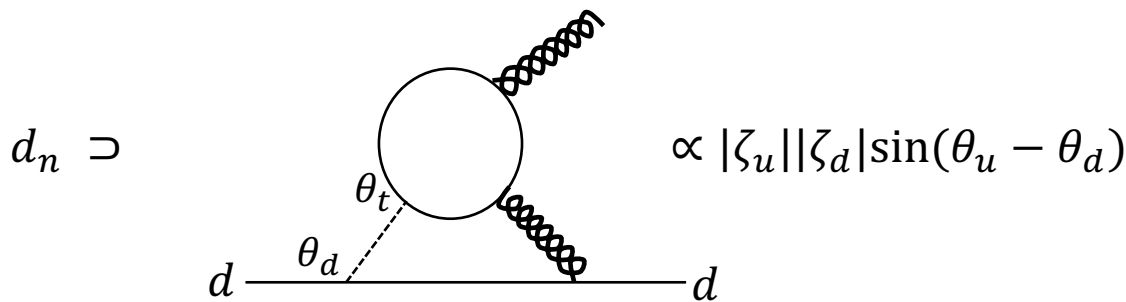
ATLAS-CONF-2020-026

Neutron EDM

Experimental bound: $|d_n| < 1.8 \times 10^{-26} e \text{ cm}$ *Abel et al. [nEDM] Phys. Rev. Lett. 124 (2020)*

ζ_d is restricted from neutron EDM.

The leading graph is chromo Barr-Zee type of down quark.



Also, from Weinberg operator $d_n(C_W) \propto |\zeta_u||\zeta_d|\sin(\theta_u - \theta_d)$,
but the sign of $d_n(C_W)$ is not determined.

Solid: current
Dashed: expected

Red: $d_n^{\text{BZ}} + d_n(C_W)$ case
Gray: $d_n^{\text{BZ}} - d_n(C_W)$ case

Destructive interference

Dimension 5 effective operator

$$H_{\text{EDM}} = -d_f \frac{\mathbf{S}}{|\mathbf{S}|} \cdot \mathbf{E} \quad \mathcal{L}_{\text{EDM}} = -\frac{d_f}{2} \bar{f} \sigma^{\mu\nu} (i\gamma_5) f F_{\mu\nu}$$

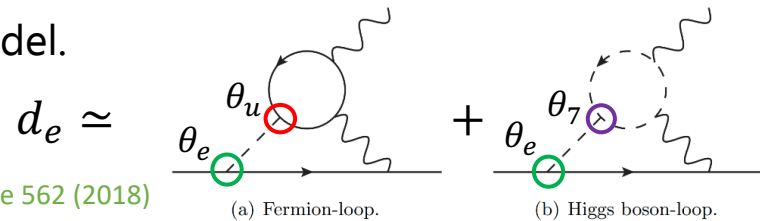
Time reversal

$$\mathcal{T}(\mathbf{E}) = \mathbf{E}, \mathcal{T}(\mathbf{S}) = -\mathbf{S} \quad \text{T violation} \rightarrow \text{From CPT theorem, CP is violated.}$$

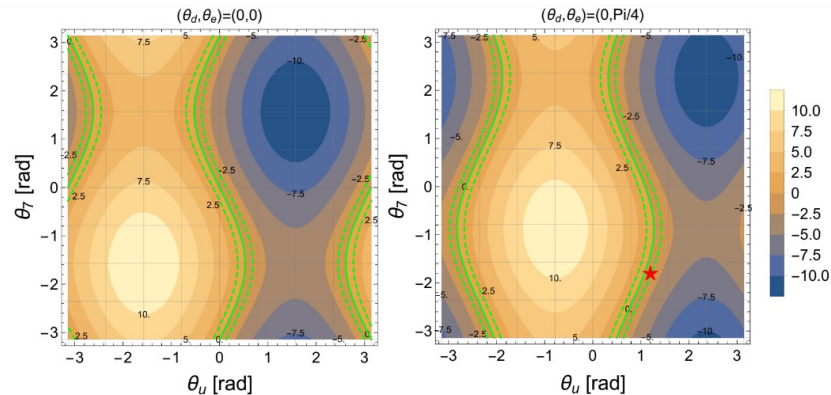
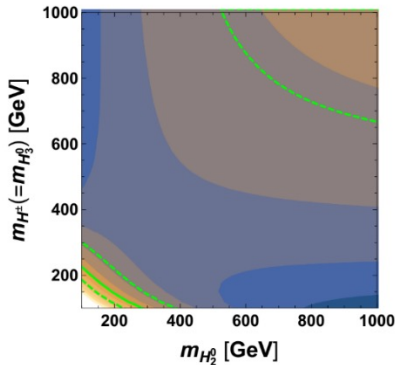
Two diagrams contribute to the electron EDM in our model.

Experimental bound $|d_e| < 1.1 \times 10^{-29} e \text{ cm}$

Andreev *et al.* [ACME] Nature 562 (2018)



Destructive interference between two independent CP phase Kanemura, Kubota and Yagyu, JHEP 08 (2020)

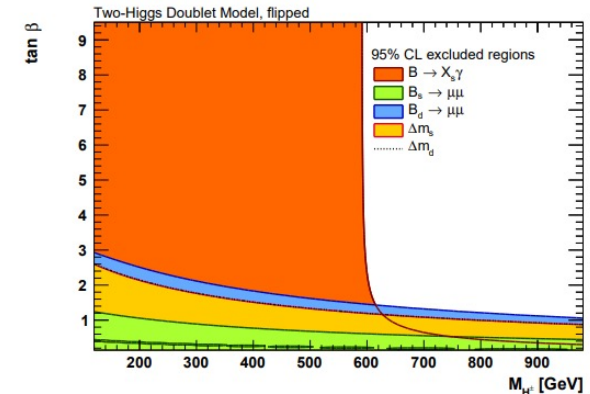
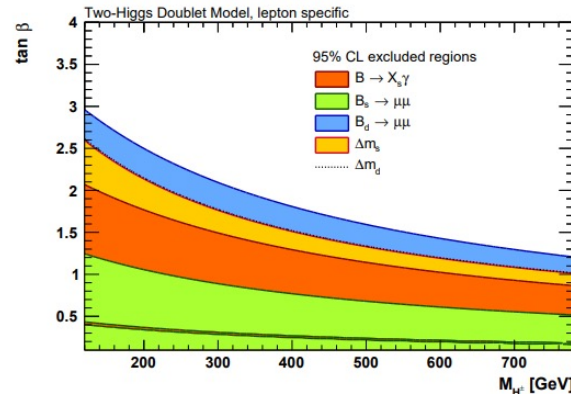
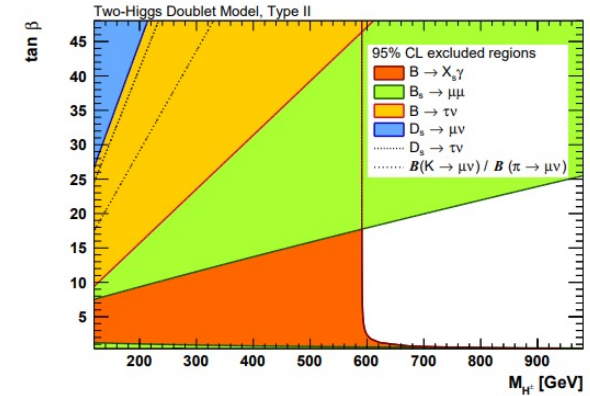
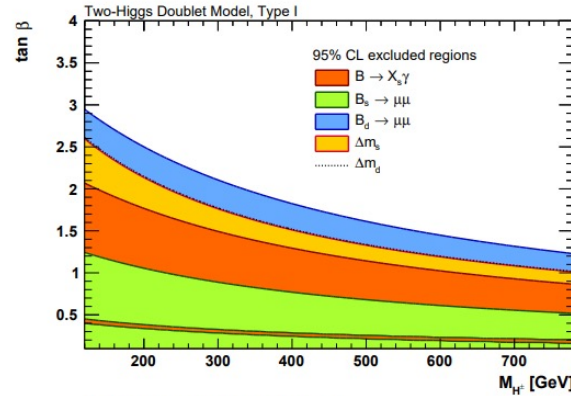


θ_7 and θ_u are important to generate BAU.

Flavor constraints

Model	ζ_d	ζ_u	ζ_l
Type I	$\cot \beta$	$\cot \beta$	$\cot \beta$
Type II	$-\tan \beta$	$\cot \beta$	$-\tan \beta$
Type X	$\cot \beta$	$\cot \beta$	$-\tan \beta$
Type Y	$-\tan \beta$	$\cot \beta$	$\cot \beta$
Inert	0	0	0

Haller *et al.* Eur. Phys. J. C 78 (2018);



Type I like

$$|\zeta_u| = |\zeta_d| = |\zeta_e| = \cot \beta$$

Type X like

$$|\zeta_u| = |\zeta_d| = \cot \beta$$

$$|\zeta_e| = -\tan \beta$$

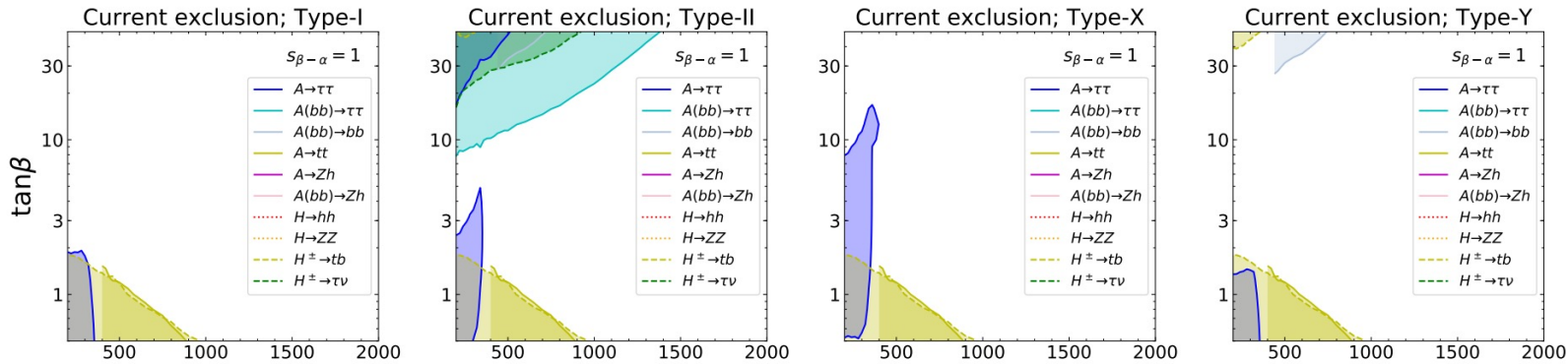
$$m_{H^\pm} \simeq 300 \text{ GeV}, |\zeta_u| \lesssim 0.4$$

Collider constraints

Aiko, Kanemura, Kikuchi, Mawatari, Sakurai and Yagyu, Nucl. Phys. B 966 (2020)

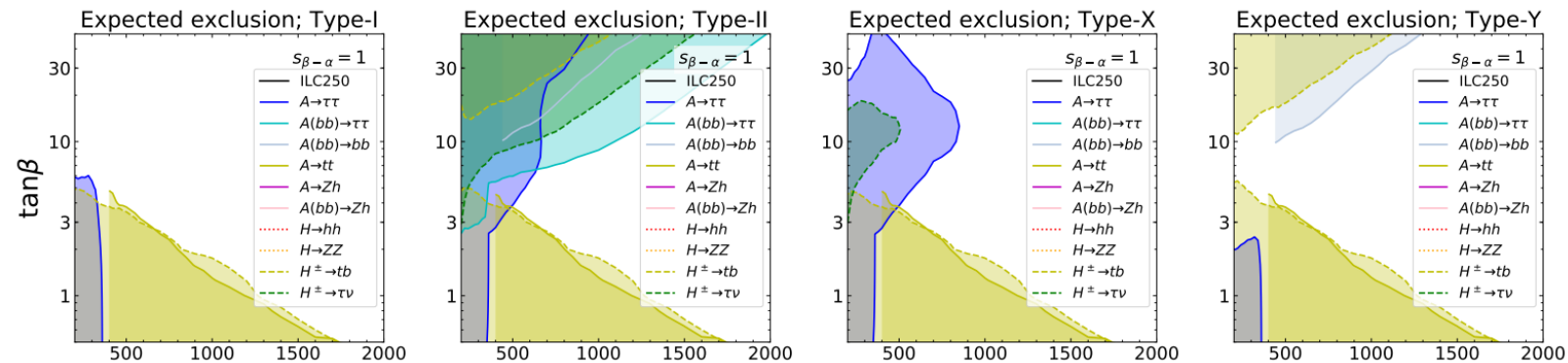
Model	S_d	S_u	S_l
Type I	$\cot \beta$	$\cot \beta$	$\cot \beta$
Type II	$-\tan \beta$	$\cot \beta$	$-\tan \beta$
Type X	$\cot \beta$	$\cot \beta$	$-\tan \beta$
Type Y	$-\tan \beta$	$\cot \beta$	$\cot \beta$
Inert	0	0	0

Current



$H_{2,3} \rightarrow \tau\tau$
 $H_{2,3} \rightarrow tt$
 $H^\pm \rightarrow tb$

HL-LHC



Multi lepton search

Kanemura, Takeuchi and Yagyū, Phys. Rev. D 105 (2022)

$\zeta_u = 0.1$ case

330 GeV

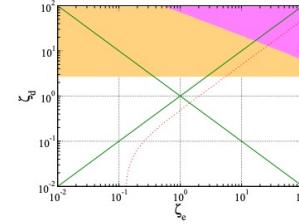
Orange: $B \rightarrow X_S + \gamma$

Magenta: $B_s \rightarrow \mu\mu$

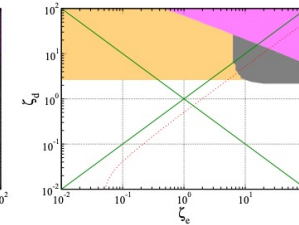
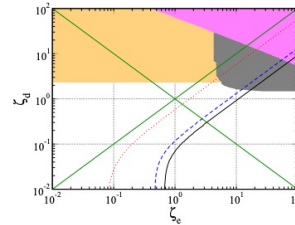
Cyan: leptonic tau decay

Black shaded: $H \rightarrow \tau\tau$

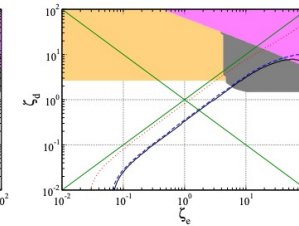
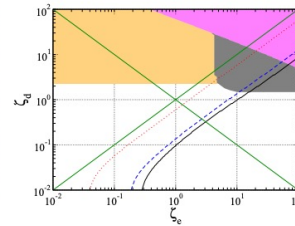
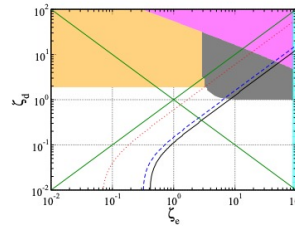
Black curves: multi lepton search



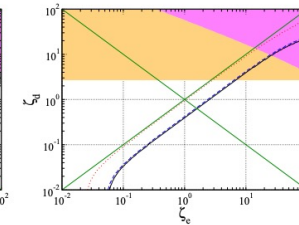
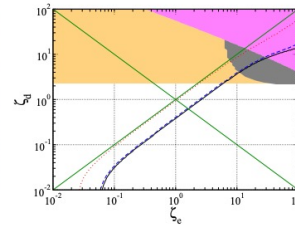
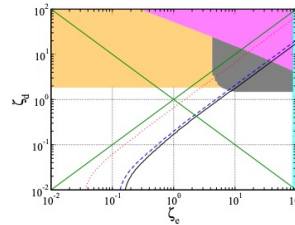
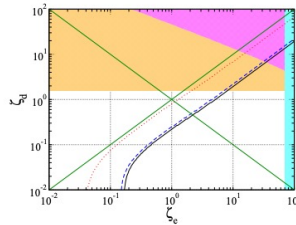
280 GeV



230 GeV



$m_{H_2} = 180$ GeV



$m_{H_3} = m_{H^\pm} = 180$ GeV

230 GeV

280 GeV

330 GeV

Other constraints

STU parameter

Considering **Higgs alignment** and $m_{H_3} = m_{H^\pm}$, our potential has custodial symmetry at 1 loop level.

$$\begin{aligned}
 V = & -\frac{1}{2}\mu_1^2 \text{Tr}(M_1^\dagger M_1) - \frac{1}{2}\mu_2^2 \text{Tr}(M_2^\dagger M_2) - \mu_{3R}^2 \text{Tr}(M_1^\dagger M_2) + \mu_{3I}^2 \text{Tr}(M_1^\dagger M_2 \tau_3) && \text{Pomarol and Vega, Nucl. Phys. B 413 (1994)} \\
 & + \frac{1}{8}\lambda_1 \text{Tr}^2(M_1^\dagger M_1) + \frac{1}{8}\lambda_2 \text{Tr}^2(M_2^\dagger M_2) + \frac{1}{4}\lambda_3 \text{Tr}(M_1^\dagger M_1) \text{Tr}(M_2^\dagger M_2) \\
 & + \frac{1}{2}\lambda_{5R} \text{Tr}^2(M_1^\dagger M_2) + \frac{1}{4}(\lambda_4 - \lambda_{5R}) \left(\text{Tr}^2(M_1^\dagger M_2) - \text{Tr}^2(M_1^\dagger M_2 \tau_3) \right) + \frac{1}{2}\lambda_{5I} \text{Tr}(M_1^\dagger M_2) \text{Tr}(M_1^\dagger M_2 \tau_3) \\
 & + \lambda_{6R} \text{Tr}(M_1^\dagger M_1) \text{Tr}(M_1^\dagger M_2) + \lambda_{6I} \text{Tr}(M_1^\dagger M_1) \text{Tr}(M_1^\dagger M_2 \tau_3) \\
 & + \lambda_{7R} \text{Tr}(M_2^\dagger M_2) \text{Tr}(M_1^\dagger M_2) + \lambda_{7I} \text{Tr}(M_2^\dagger M_2) \text{Tr}(M_1^\dagger M_2 \tau_3) && \rightarrow T = 0
 \end{aligned}$$

S and U parameter in general CPV 2HDM [Haber and Neil, Phys. Rev. D 83 \(2011\)](#)



S and U are very small in our benchmark scenario.

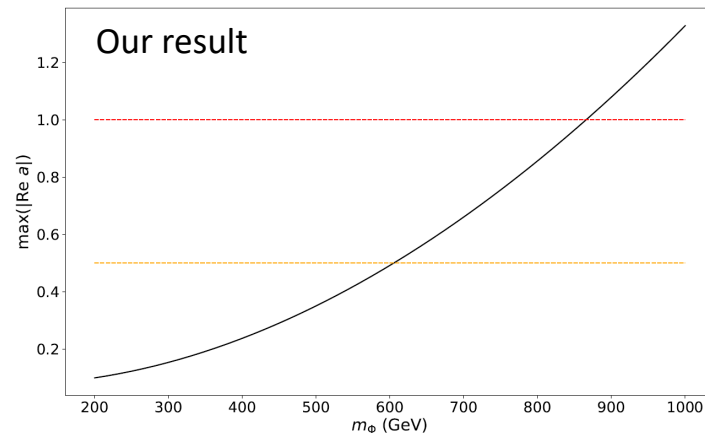
Bounded from below

[Ferreira, Santos and Barroso, Phys. Lett. B 603 \(2004\)](#)

$$\begin{aligned}
 \lambda_1 & \geq 0, \quad \lambda_2 \geq 0 \\
 \lambda_3 & \geq -\sqrt{\lambda_1 \lambda_2}, \quad \lambda_3 + \lambda_4 \mp \lambda_{5R} \geq -\sqrt{\lambda_1 \lambda_2} \\
 |\lambda_{7R}| & \leq \frac{1}{4}(\lambda_1 + \lambda_2) + \frac{1}{2}(\lambda_3 + \lambda_4 + \lambda_{5R}) \\
 |\lambda_{7I}| & \leq \frac{1}{4}(\lambda_1 + \lambda_2) + \frac{1}{2}(\lambda_3 + \lambda_4 - \lambda_{5R})
 \end{aligned}$$

Unitarity bound (M = 30 GeV)

[Kanemura and Yagyu, Phys. Lett. B 751 \(2015\)](#)



Shape of the chemical potential

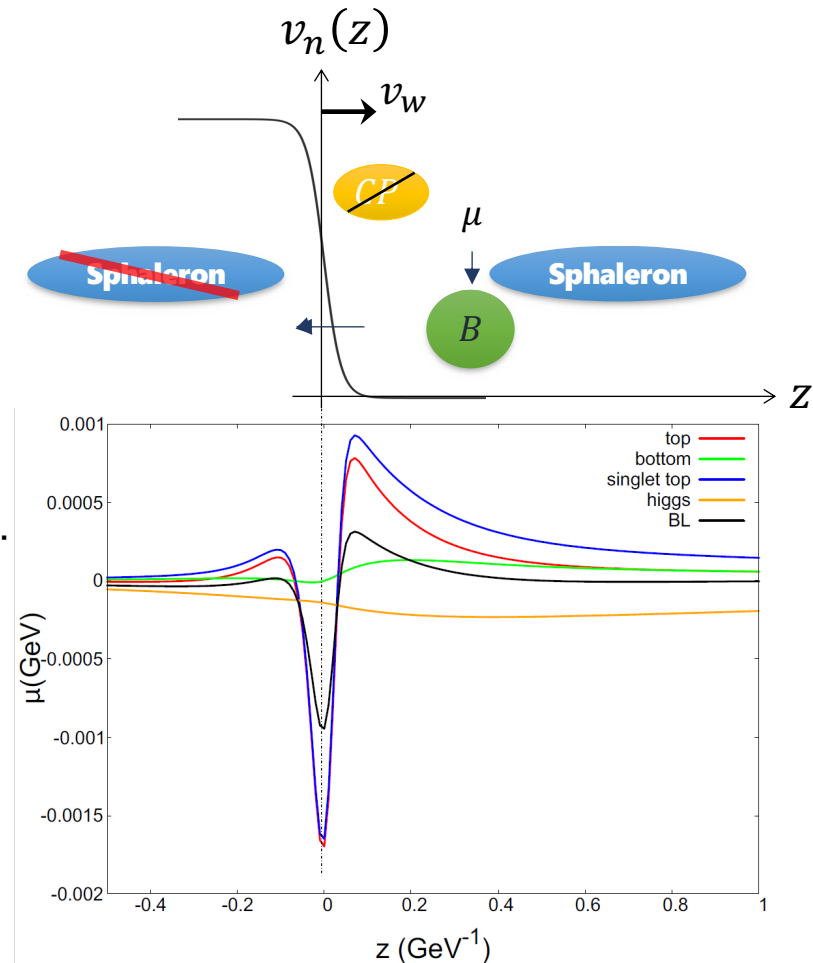
When the top transport scenario, θ_7 and θ_u are important for the BAU.

Localized mass around the wall

$$m_t(z) = \frac{y_t}{\sqrt{2}} v(z) e^{i\theta(z)}$$

makes chemical potential.

$v(z), \theta(z), T_n$, etc.
depend on models and dynamics of PT.



About Landau pole

EWPT and triviality bound

- Effective potential with high T expansion

$$V_{eff}(\varphi, T) = D(T^2 - T_0^2) - ET|\varphi|^3 + \frac{\lambda_T}{4}\varphi^4$$

- Non-decoupling effect of heavy scalars

Ex) Two Higgs Doublet Model (2HDM)

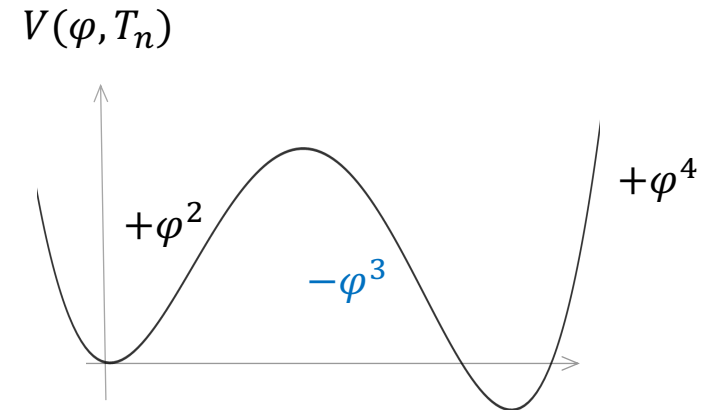
$$m_{\Phi}^2 = M^2 + \tilde{\lambda}v^2 \simeq \tilde{\lambda}v^2 \quad (\tilde{\lambda}v^2 \gg M^2)$$

$$E \simeq \frac{1}{4\pi v^3} (m_W^3 + m_Z^3 + m_{\Phi}^3) \sim g^{3/2} + \tilde{\lambda}^{3/2}$$

- Large scalar self couplings are needed for strongly first order PT.

From RGE analysis, Landau pole appears around 1-100 TeV.

Triviality bound : $\Lambda \lesssim 3 \text{ TeV}$



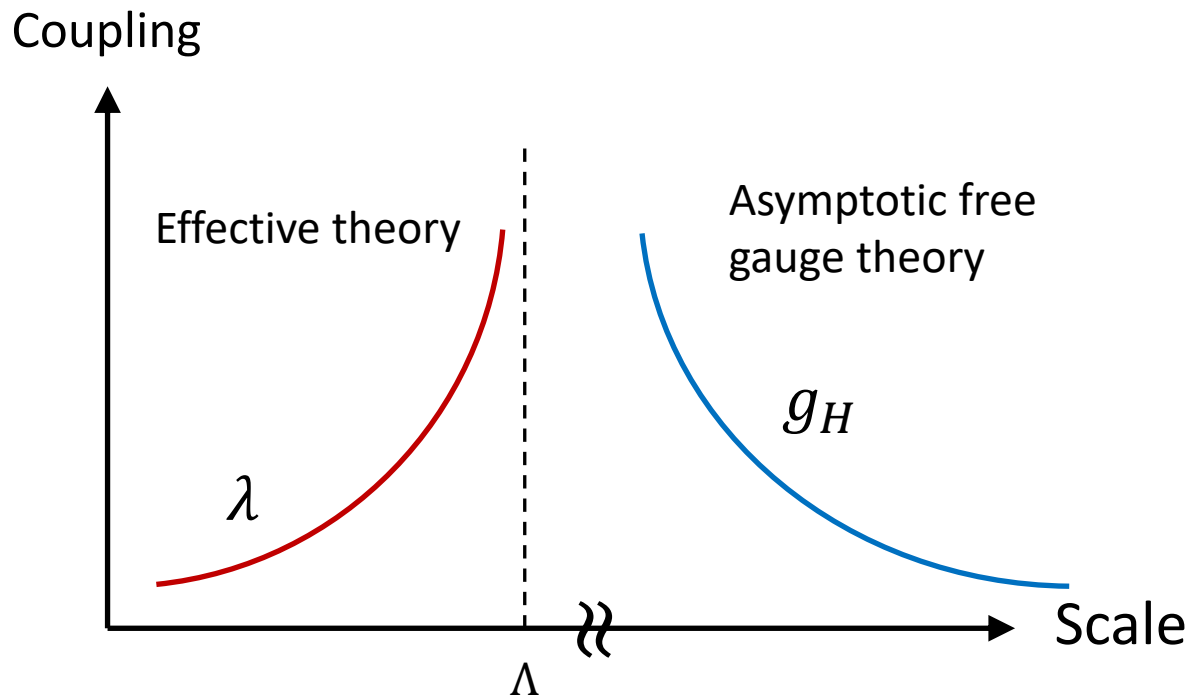
Cline, Kainulainen and Trott (2011); Kanemura, Senaha and Shindou (2011);
Kanemura, Senaha, Shindou and Yamada (2013); Dorsch, Huber, Konstandin and No (2017); and more

Beyond Landau pole

A new theory is needed above Landau pole.

Ex) Minimal SUSY fat Higgs model [Harnik, Kribs, Larson and Murayama \(2004\)](#)

At the high scale above Landau pole,
scalar couplings behave as non-Abelian gauge couplings



Scalar bosons are meson states as a result of confinement like QCD.

RGE analysis

- Scalar self couplings in aligned 2HDM

$$\lambda_1, \lambda_2, \lambda_3, \lambda_4, \lambda_5$$

$$\text{Re}[\lambda_6], \text{Im}[\lambda_6], \text{Re}[\lambda_7], \text{Im}[\lambda_7]$$

- Beta function with dim. reg + $\overline{\text{MS}}$ scheme (at 1 loop level)

- Consider threshold effect

Dorsch, Huber, Konstandin and No (2017)

From SM beta function to a2HDM beta function

- At matching scale,

$$\lambda_i^{\text{SM}}(\tilde{\mu}) = \lambda_i^{\text{A2HDM}}(\tilde{\mu}) \quad (i = 1 \dots 7)$$

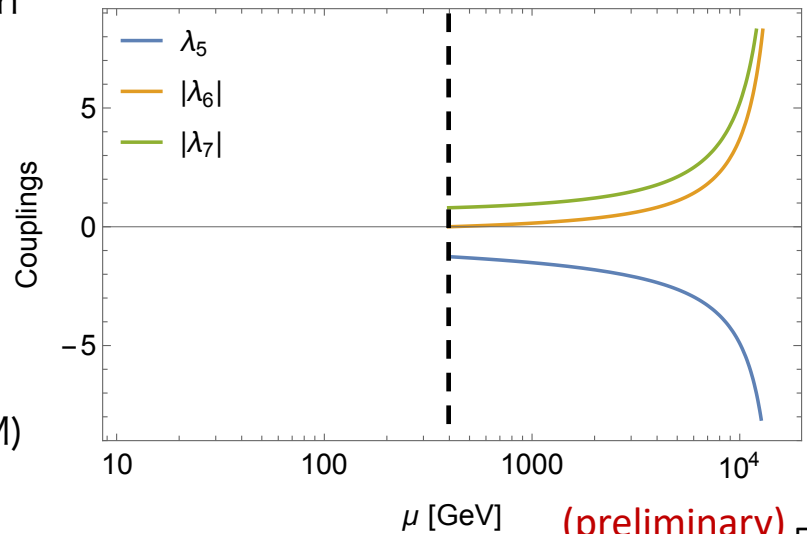
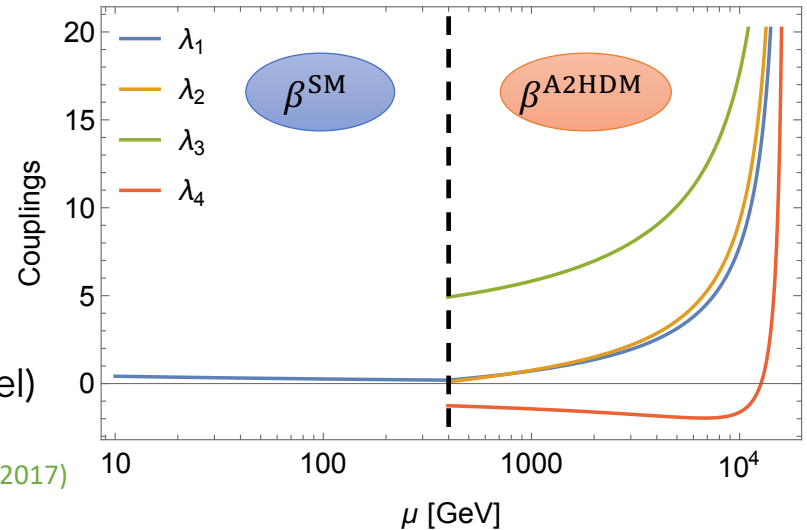
$$\tilde{\mu} = \max\{m_{H_2}, m_{H^\pm}\}$$

No threshold effect

⇒ Landau pole appears around 1-3 TeV (2HDM)

Cline, Kainulainen and Trott (2011)

Scale dependences of couplings (BP1)



RGE analysis

- Self-couplings become non-perturbative at $\Lambda_{4\pi}$.

$$\max\{\lambda_i\} > 4\pi \quad (i = 1 \dots 7)$$

- Strength of PT and v_n/T_n

▼ BP1

$$m_{H_2} = 267 \text{ GeV}$$

$$m_{H_3} = m_{H^\pm} = 381 \text{ GeV}$$

$$M = 30 \text{ GeV}$$

$$\Lambda_{4\pi} = 6.7 \text{ TeV}$$

◆ BP2

$$m_{H_2} = 397 \text{ GeV}$$

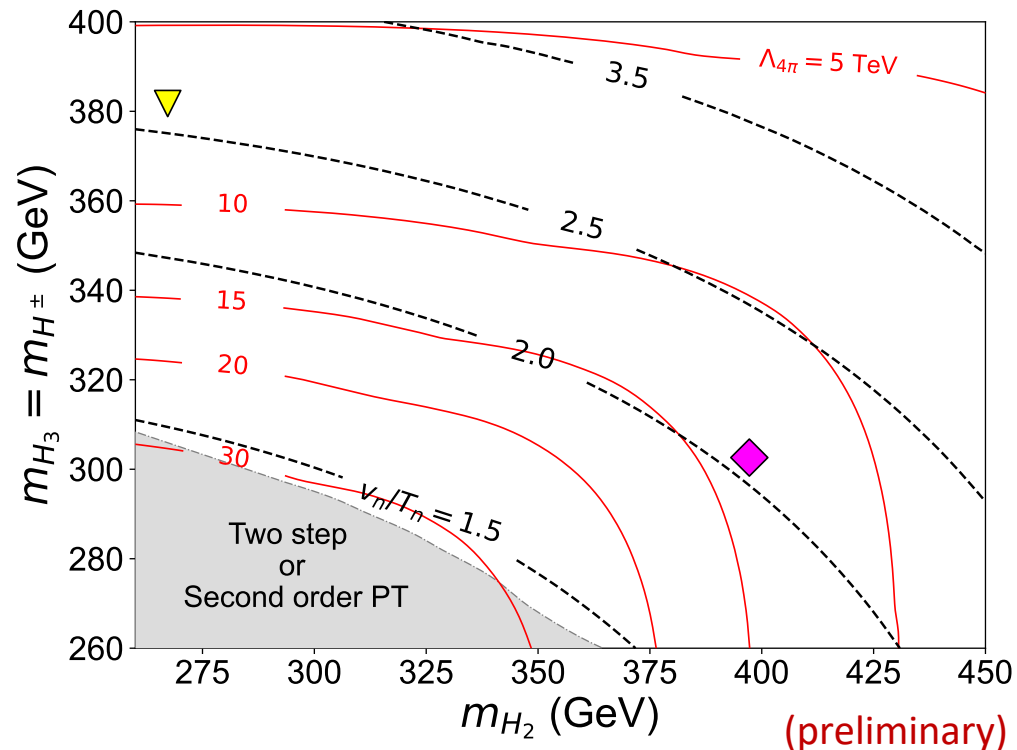
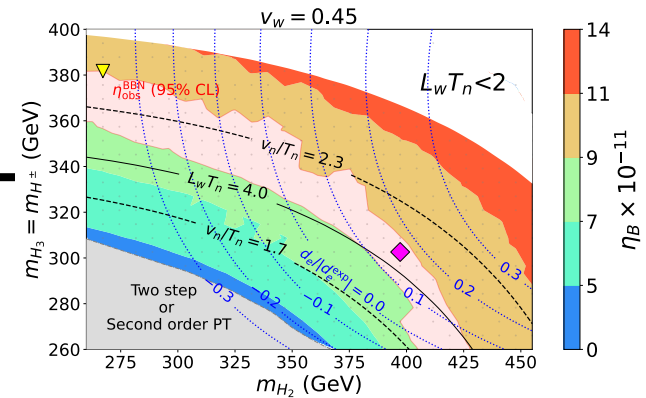
$$m_{H_3} = m_{H^\pm} = 302 \text{ GeV}$$

$$M = 30 \text{ GeV}$$

$$\Lambda_{4\pi} = 13.4 \text{ TeV}$$

- Benchmark points for GW signal

Landau pole appear around $\Lambda_{4\pi} = O(10)$ TeV



▼ BP1: Strong PT

◆ BP2: Weak PT